ANL-6658

ANL-6658

Argonne National Laboratory

REACTOR DEVELOPMENT PROGRAM PROGRESS REPORT

November 1962

ANL-6658
Reactor Technology
(TID-4500, 18th Ed.)
AEC Research and
Development Report

ARGONNE NATIONAL LABORATORY
9700 South Cass Avenue
Argonne, Illinois

REACTOR DEVELOPMENT PROGRAM PROGRESS REPORT

November 1962

Albert V. Crewe, Laboratory Director

Division	Director
Chemical Engineering	S. Lawroski
Idaho	M. Novick
Metallurgy	F. G. Foote
Reactor Engineering	B. I. Spinrad
Remote Control	R. C. Goertz

Report coordinated by R. M. Adams

Issued December 15, 1962

Operated by The University of Chicago
under
Contract W-31-109-eng-38
with the
U. S. Atomic Energy Commission

FOREWORD

The Reactor Development Program Progress Report, issued monthly, is intended to be a means of reporting those items of significant technical progress which have occurred in both the specific reactor projects and the general engineering research and development programs. The report is organized in a way which, it is hoped, gives the clearest, most logical over-all view of progress. The budget classification is followed only in broad outline, and no attempt is made to report separately on each sub-activity number. Further, since the intent is to report only items of significant progress, not all activities are reported each month. In order to issue this report as soon as possible after the end of the month editorial work must necessarily be limited. Also, since this is an informal progress report, the results and data presented should be understood to be preliminary and subject to change unless otherwise stated.

The issuance of these reports is not intended to constitute publication in any sense of the word. Final results either will be submitted for publication in regular professional journals or will be published in the form of ANL topical reports.

The last six reports issued in this series are:

May 1962	ANL-6573
June 1962	ANL-6580
July 1962	ANL-6597
August 1962	ANL-6610
September 1962	ANL-6619
October 1962	ANL-6635

TABLE OF CONTENTS

TABLE OF CONTENTS

TABLE OF CONTENTS

I. WATER-COOLED REACTORS

A. EBWR

The results of the month's principal activities can be briefly summarized as:

(a) Achievement of the goal of reactor power output of 100 Mwt;

(b) Identification of the transition region between carryunder and carryover, and the effect of the transition on the power coefficient, water level, and power output of the EBWR reactor.

1. Physics Considerations of Operation up to 100 Mw

It was originally estimated that a 100-Mwt output could be achieved with an average of 1.57 poison strips (boron-stainless steel) per spike. This strip average, in the ring of 28 spikes, resulted in a core reactivity ρ (cold) of 10.5%.

Power-coefficient measurements made to power levels up to 60 Mw yielded the following:

$\Delta k/\Delta(Mw) \cong 0.065\% \rho/Mw$ in the range 10-40 Mw;

$\Delta k/\Delta(Mw) \cong 0.10\% \rho/Mw$ in the range 40-60 Mw.

A relative increase in required reactivity per Mw was thus noted at power levels between 40 to 60 Mw.

The measured excess reactivity required for 60-Mw operation was about 5%, corresponding to an average calculated void fraction of 20%. But the latter was also the original calculated void fraction for 100-Mw power level. It thus appeared that there was a lost component of reactivity.

Extrapolation of data indicated that 80 to 85 Mw could be obtained by the addition of 2% ρ. The additional reactivity was achieved by removing one strip from each of 16 of the 28 spikes of the central ring. This resulted in an average of one strip per spike. The nine-rod cold shutdown requirement as stated in the hazards report was met, with approximately 0.7% reactivity worth of rods still available. The reactor was operated at 80 Mw with near equilibrium xenon and produced near-dry steam. It was found that, although this required all the (~2%ρ) reactivity to reach 80 Mw, there was insufficient reactivity to reach 100 Mwt without carryover.

Powers greater than 80 Mw and as high as 100 Mw, however, were achieved by operating the reactor with increasing carryover; that is, water carried over with the steam. Thus, some additional reactivity was obtained

with this modified form of operation. To achieve this power, however, the rate of feedwater addition had to be increased to provide for the loss of water from the reactor vessel caused by carryover.

2. Hydraulics

The performance characteristics of EBWR are greatly affected by vapor-liquid separation phenomena which are of course, sensitive to the geometry of this particular system. At power levels up to approximately 65 Mw, steam carryunder in the downcomer is the controlling variable. As the power is increased to 65 Mw, the carryunder increases and reduces the subcooling, with the result that the reactivity lost in voids increases. Above 65 Mw, and dependent on the water level in the reactor vessel, the vapor velocities in the steam dome are such that liquid carryover commences and the performance characteristics of the reactor are again radically changed. As the carryover increases with increasing power above 65 Mw, the excess makeup (cold feedwater equalling the amount being carried over) provides the additional subcooling and hence reactivity to reach the higher power levels. As a result, the reactor behavior is extremely sensitive to water level, which strongly influences the liquid carryover rate.

3. Stability

EBWR stability was determined by measuring experimentally the reactor transfer function at selected power levels and extrapolating the results of these measurements linearly to obtain an upper limit for stable operation at higher powers. From measurements at 10, 20, 40, 60, and 70 Mw a maximum stable power of 85 Mw was indicated, assuming the mode of reactor operation was with negligible carryover.

Transfer function measurements were not performed at power levels above 75 Mw, but reactor behavior was investigated by calculating the autocorrelation function and power density spectrum of the neutron flux noise. This investigation was carried out up to 100 Mwt.

4. Noise Measurements

Ten experiments were performed with the EBWR at powers from 60 to 100 Mw, varying boric acid concentrations, and various rod positions, all at 600 psi, to provide noise records for evaluation of the correlation function and power density spectrum.

Instrumentation was added to the reactor console to provide a continuous indication of average neutron flux and the root-mean-square (rms) noise as a percentage of power. The percentage rms meter proved to be useful in operating the reactor because it gave a numerical indication of reactor behavior. Previously, reactor behavior was estimated from the

peak-to-peak deviations from the linear flux strip chart recorder at the reactor console. The differences in rms noise as a function of water level at constant power were clearly indicated, as well as the changes in rms noise at higher powers with constant water level.

5. Equipment and Power Determinations

Performance of the reboiler plant at high-power operation was satisfactory, considering that it had not been completely "debugged" prior to the high-power runs. Some difficulties in reboiler plant control were encountered because of the large amount of carryover. However, these difficulties were not insurmountable and controlled operation was maintained during the period of time at 100-Mw operation.

Reactor power was determined on the basis of heat balance calculations made for both the primary and intermediate systems. The heat balance data of the intermediate system were used to determine the amount of carryover in the primary steam lines. It was necessary to use the intermediate system for accurate power determinations since carryover in this system did not present a problem. The feedwater flow in the primary system was compared with the intermediate system flow in order to determine carryover.

B. BORAX-V

1. Operations and Experiments

Zero-power experiments were completed at conditions up to 600 psig and 489°F with the initial reference boiling core in BORAX-V, now designated Core B-1. This core contained 32 boron-stainless steel poison rods, the oscillator rod and assembly in core position 75, five $\frac{3}{8}$-in. stainless steel miniature ion chamber thimbles in place of fuel rods, and six $\frac{1}{8}$-in. stainless steel flux wire thimbles in coolant channels. Preliminary analysis of the results of these experiments showed a loss in available excess reactivity of about 2.2% due to installation of the oscillator rod and fuel assembly, miniature ion chamber thimbles, and flux wire thimbles. Loss in available excess reactivity due to heating from room temperature to operating conditions was about 7%. The remaining available excess reactivity at operating conditions was estimated to be about 3%.

A reduction in the differential reactivity worth of control rods was again measured upon heating the reactor without boric acid in the reactor water. The reactivity worth of the two intermediate control rods, 6 and 8, adjacent to the oscillator assembly was less than that of control rods 2 and 4 on the opposite side of the core.

Experiments were carried out with Core B-1 which indicated that the position of the Sb-Be neutron source, at either 15 in. (entirely removed from beryllium) or fully inserted into the reactor, had a negligible effect

on the results of reactivity measurements during the hot critical operation. This indicated that, at power levels necessary for satisfactory nuclear instrument performance, the withdrawal of the source is not necessary.

Equipment for measuring the transfer function of BORAX-V through cross correlation was checked out at zero power and found to work satisfactorily.

Since the available excess reactivity in Core B-1 was not considered sufficient to achieve rated power of 20 Mwt, the reference core has been changed by replacing four fuel rods in 59 fuel assemblies with water-filled X-8001 aluminum "flow" rods to increase the water-fuel ratio. This new core is designated boiling Core B-2. It is expected that this change will flatten the neutron-flux distribution within each fuel assembly, reduce the reactivity effects of both temperature and steam voids, and thus increase the available excess reactivity. The number and location of boron-stainless steel poison rods were adjusted to satisfy the "one-stuck-control-rod" criterion. Boiling Core B-2 contains 33 poison rods, five stainless steel miniature ion chamber thimbles, 236 flow rods, and an oscillator rod assembly. The change resulted in a reactivity increase at room temperature of about 0.64% $\Delta k/k$ as compared with the final configuration of Core B-1. The loading diagram for Core B-2 is shown in Figure 1.

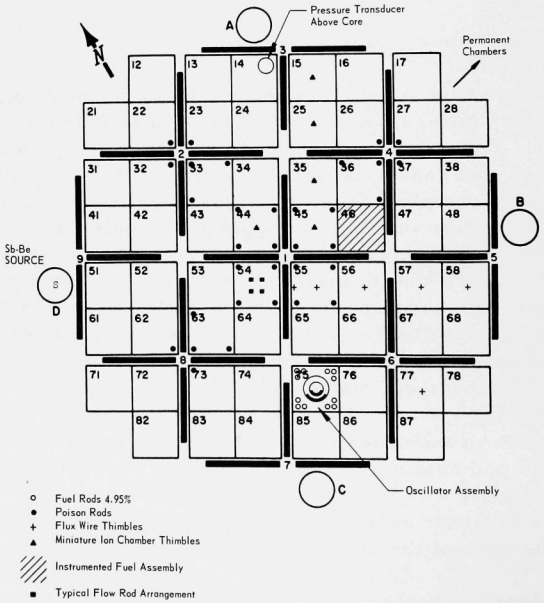

Figure 1. Loading Diagram - Boiling Core B-2 - BORAX-V

One instrumented boiling assembly was installed in the reactor. The oscillator, pressure transducer, and downcomer flow and density instruments remain in the same positions used for boiling Core B-1.

Two attempts to increase reactivity in Core B-2 by spiking with 9.9% enriched fuel rods in the low neutron-flux regions of three fuel assemblies near a corner of the core were unsatisfactory because of the probable violation of the "one-stuck-control-rod" criterion on the adjacent intermediate control rod, accompanied by only a very minor gain in reactivity. This approach was discontinued and all 9.9% enriched fuel rods removed.

A gold flux wire irradiation was carried out to measure neutron-flux distribution along a NE-SW diametral traverse across the core on a plane below the control rod bank, $4\frac{1}{2}$ in. above the bottom of the core. This measurement confirmed that the neutron-flux distribution is tilted, being lower on the side of the core containing the oscillator.

Two experiments were run to determine the differential reactivity worth of a fueled oscillator in the reflector of Core B-2 at room-temperature conditions. A $2\frac{3}{4}$-in.-diameter by 25-in.-long rotor consisting of 180° of 0.040-in.-thick cadmium and 180° of Al-U fuel plate containing 16 g of U^{235} when located in instrument thimble A had a differential worth of about 0.066% $\Delta k/k$. The same configuration containing 55 g of U^{235} measured about 0.11% $\Delta k/k$. This compares with the measured differential reactivity worth of about 0.1% at room temperature for the present shadow-type oscillator located in core position 75.

2. Modification and Maintenance

A modification was made in the method of retaining the feedwater sparger in position. There had been vibration of the sparger, indicated by marks on the bent support feet. A bracket from the core structure struts was installed to hold down the sparger.

The turbine-type flowmeter coils on instrumented boiling fuel assembly I-2 have been replaced with new coils which also incorporate a brazed joint between the Inconel extension wire sheath and the Type 304 stainless steel coil housing. The coils were leak-tested and installed on the assembly, and the flowmeters were recalibrated in the air-water test loop. The instrumented assembly is now installed in the reactor in preparation for power operation of the core.

A temperature-control system for the continuous chloride analyzer has been constructed and tested. It maintains the analyzer temperature at 69° ± 1°F, which is considered satisfactory for accurate analysis.

A new piping manifold for operating the makeup-water demineralizer has been installed to eliminate the defects and limitations of the existing equipment.

3. Analysis

A calculation of a somewhat simplified theoretical BORAX-V transfer function ($\Delta n/n_0 \Delta k_{ex}$) at 20 Mwt is being calculated with the IBM-704 for several values of void and Doppler coefficients of reactivity. After this preliminary study is completed, a calculation of the frequency response of a more elaborate model will be made at several power levels.

Also, a simplified version of the reactor model is being set up on a 10-amplifier Donner analog computer (Model 3400). The effects of void and Doppler coefficients and the nonlinearity of the kinetics equations are being investigated.

Calculations are also proceeding on the IBM-1620 computer to determine the steady-state relationship between average void fraction, power level, and steam carryunder in BORAX-V. An initial set of calculations for zero carryunder has been completed.

An effort is being made to interpret the measured loss of differential worth of the control rods in Core B-1 under hot conditions. PDQ control cell problems have been prepared for hot and cold conditions to obtain neutron-flux distributions adjacent to the control rods. This study is to check the theory that a reduction in neutron-flux peaking in control rod channels, expected when the reactor is heated, could cause a reduction in control rod worth. Other theories are also being investigated.

4. Design

A conceptual design study has started on advanced superheater fuel elements, with the objectives of improved performance and fabricability, and reduced fuel cost. Currently, designs using rod- and pellet-type fuel elements are being studied.

Detail design has started on the new step-function generator. This design incorporates an air cylinder stepping an intermediate control rod for a distance of 5 in. from any point on the rod stroke. A new rod drive mechanism, using the existing seal and scram latch, is required.

The superheater fuel storage rack has been redesigned to provide a greater margin of safety.

A preliminary design has been made to convert the turbine-type, in-core flowmeter coil from a self-generating device to a variable-reluctance device. The original basic turbine body is utilized, but the blade tip and coil construction are modified to provide an axial magnetic flux path. It is planned to check the design at room temperature with a dummy flowmeter, using a high-permeability magnetic material (Carpenter "HYMU-80").

5. Procurement and Fabrication

a. Superheater Fuel. The status of fuel fabrication for the BORAX-V Superheat Core is given in Table I. During the month, two central instrumented and seven standard peripheral subassemblies were brazed. Welding operations were completed on the last six standard central fuel elements, and these are currently being straightened and inspected.

Table I. Status of BORAX-V Superheat Fuel Fabrication

	Central Type		Peripheral Type	
	Standard	Instrumented	Standard	Instrumented
Subassemblies Required	71	9	89	6
Subassemblies Brazed	71	7	91	0
Subassemblies to be Brazed	0	2	0 (2 Rejects)	6
Assemblies Required	13	3	17	2
Assemblies Completed	13	0	12	0
Assemblies to be Completed	0	3	5	2
Elements Completed	13	0	0	0
Elements to be Completed	0	3	17	2

Welding assembly was completed on two instrumented central superheater fuel assemblies. A total of 95 four-plate fuel elements for the peripheral superheater have been brazed, including six thermocouple elements. This completes the vacuum-brazing operation, using Coast Metals-60 brazing alloy, on all peripheral elements.

b. Experimental Components. The replacement of aluminum rivets with Type "A" nickel rivets in instrumented boiling fuel assembly I-1 has been completed. Brazing assembly and installation of flowmeter coils is proceeding.

6. Development and Testing

a. Advanced Superheater Fuel. An addendum to the original BORAX-V superheater fuel plate fabrication contract with Atomics International has been let, providing for the fabrication of 25 HCE-406 and 25 FCE-406 fuel plates. These plates, made of a highly enriched UO_2-Type 406 stainless steel cermet, clad with Type 406 stainless steel, will be used to make two experimental superheater fuel assemblies similar to the present reference design.

Type 406 stainless steel material has been procured by the Laboratory and fabrication has started on components of developmental fuel plates.

b. Boiling Fuel Assembly. A boiling fuel assembly box containing 49 dummy stainless steel fuel rods is being autoclaved at 600-psig, saturated conditions to determine the reliability of the new "A" nickel rivets which replaced the failed X-8001 aluminum rivets that fastened the stainless steel upper and lower grids to the X-8001 aluminum fuel assembly box. Inspection after three weeks in the autoclave revealed no sign of rivet or box failure and negligible corrosion of the "A" nickel rivets. The test is continuing.

c. In-core Instrumentation. In attempting to find an easier means of sealing multiple instrument leads against steam at 600 psi and 489°F, high-temperature potting resins have been investigated. A formulation based on Dow Chemical Company's Novolac resins "D.E.N. 438" and "D.E.R. 337" was cast for testing. The material is recommended for temperatures up to 500°F in air atmospheres; however, a one-week test of samples in water at 489°F produced complete failure. The material was reduced to a group of gray, clinker-like fragments.

Samples of Shell Oil Company's "Epon 828" were tested at the same time. This material also failed, but was converted to a thick slurry rather than breaking up as did the other material.

II. LIQUID-METAL-COOLED REACTORS

A. General Research and Development

1. ZPR-III

Experiments continued with Assembly 41, a dilute metal system with a 5-to-1 ratio for U^{238}/U^{235}, (see Progress Report, Sept 1962, ANL-6619). Results of the radial reflector experiments done in October with steel and aluminum (see Progress Report, Oct 1962, ANL-6635, p. 13) were confirmed. Additional radial reflector experiments were done with a composition similar to the EBR-II blankets, and flux traverses were obtained radially at the reactor midplane. Fission rate traverses were also made along the core axis and at the core radial edge. Some further central fission ratio measurements were made, as well as more investigation of sample-size effects in central reactivity measurements.

a. Steel and Aluminum Radial Reflector Experiments. A series of radial reflector experiments was performed in the radial blanket region around one quadrant of the core in one machine half. Substitutions of aluminum were made for the regular depleted uranium loading in three successive rows of blanket drawers, or matrix tubes, around the core sector. The substitutions were repeated with Type 304 stainless steel. An additional experiment with a half row aluminum reflector was also done. Reactivity worths of various thicknesses of steel and aluminum reflectors replacing depleted uranium blanket were thereby obtained. The results, extrapolated to a full reflector around the circumference of the basic critical core for this assembly (see September, 1962, Monthly Report, ANL-6619), are given in Table II. An initial positive worth for aluminum is seen to give way to negative worth with increased thickness, presumably due to a leakage effect.

Table II. Steel and Aluminum Radial Reflector Experiments

Reflector or Blanket Type	Composition, Volume %			Average Reflector Thickness (in.)*	Worth, Replacing Depleted Uranium Around Entire Core Circumference (Ih)	
	Depleted Uranium	Stainless Steel	Aluminum		Steel Reflector	Aluminum Reflector
Depleted Uranium	84	9	-	1.37	-	+14
Aluminum	-	9	84	2.72	+310	+2
Stainless Steel	-	93	-	5.40	+518	-28
				8.00	+576	-101

*Established on a cross-sectional area basis.

b. Central Fission Ratios. Some additional fission ratio measurements were made at the core center in order to clarify some anomalies noted in previous measurements and reported previously (see Progress Report, Oct 1962, ANL-6635, p. 8). Three types of counters have been used in these measurements, all with a basic design described by Kirn.[1] In the original Kirn chambers, a heavy-wall construction was used and the operating gas was sealed in. Two types of gas flow counters also were used in which the fissile platings were on replaceable foils; one type had a heavy-wall construction, similar to the old Kirn counters, the other used a wall as thin as practical. Fission rates for the threshold isotopes are sensitive to wall thickness because of the inelastic scattering, a problem investigated by Davey.[2]

Fission ratios were measured in the heavy-walled gas-flow counters with foils of enriched uranium, natural uranium, and U^{236} to compare with previous measurements made with the same foils in the thin-walled gas-flow counters, and the Kirn chamber ratios. For the U^{236}/U^{235} ratio, the value obtained by means of the heavy-walled counters was 5% lower than in thin-walled counters, a result somewhat anticipated. However, the U^{236}/U^{235} ratio is 15% smaller in the heavy-walled counters than the same ratio found with the older Kirn counters. Resolution of this anomaly awaits the development of radiochemical analytical equipment at EBR-II for re-examining the strength of the stock solutions used in preparation of the counter foils. The U^{238}/U^{235} ratios obtained with the natural and enriched uranium foils in the thin-walled and the heavy-walled counters differ by 4%. However, the U^{238}/U^{235} ratio found with the Kirn counters appears to be 3% lower than with the heavy-walled counters. Table III gives a summary of these recent measurements.

Table III. U^{236}/U^{235} and U^{238}/U^{235} Fission Ratios with Thin-walled Gas-flow, Heavy-walled Gas-flow, and Kirn Counters

Measurement No., Ratio	Counters Used	Foils Used	Ratio Value
U^{236}/U^{235}	Thin-wall, gas flow	U^{236} #27 - U^{235} #2	0.0895
U^{236}/U^{235}	Heavy-wall, gas flow	U^{236} #27 - U^{235} #2	0.0847
U^{236}/U^{235}	Kirn Counters #24 and 5	U^{236} - U^{235}	0.1103
U^{238}/U^{235}	Thin-wall, gas flow	Nat. U #2 - U^{235}	0.0392
U^{238}/U^{235}	Heavy-wall, gas flow	Nat. U #2 - U^{235}	0.0377
U^{238}/U^{235}	Kirn Counters #2 and 5	Depl. U - U^{235}	0.0366

[1] F. S. Kirn, An Absolute Fission Counter, ANS Second Winter Meeting (1957).

[2] W. G. Davey, A Critical Comparison of Measured and Calculated Fission Ratios for ZPR-III Assemblies, ANL-6617 (Sept 1962).

c. Central Reactivity Measurements with Enriched Boron Carbide. Continued investigations were made of the effects of sample size in reactivity coefficient measurements with high-capture materials. Of particular interest is the sensitivity of the measurements to the sample arrangement in the sample space. One series of measurements was made in a 2 x 2 x 2-in. central sample space using one to four layers of $\frac{1}{4}$ x 2 x 2-in., enriched B_4C stacked up in the space. The four layers were also dispersed in the sample space, using interspacing layers of empty steel cans. Table IV gives the results. Experiments were then done in $\frac{1}{4}$ to 1 x 2 x 2-in. sample spaces where the entire space was filled with enriched B_4C. The worths of these samples are also given in Table IV. The data show variations of worth, due to sample size and arrangements, of up to 20 percent.

Table IV. Central Reactivity Worths of Enriched B_4C Samples

Sample Space (in.)	Arrangement of Enriched B_4C	Weight Enriched B_4C* (g)	Reactivity Coefficient Ih/g
2 x 2 x 2	$\frac{1}{4}$ x 2 x 2-in. layer	32.8	1.01
2 x 2 x 2	$\frac{1}{2}$ x 2 x 2-in. layer	64.0	0.95
2 x 2 x 2	$\frac{3}{4}$ x 2 x 2-in. layer	96.2	0.89
2 x 2 x 2	1 x 2 x 2-in. layer	128.2	0.86
2 x 2 x 2	4 dispersed $\frac{1}{4}$ x 2 x 2-in. layers	128.2	0.92
$\frac{1}{4}$ x 2 x 2	$\frac{1}{4}$ x 2 x 2 in.	31.5	1.05
$\frac{1}{2}$ x 2 x 2	$\frac{1}{2}$ x 2 x 2 in.	64.0	0.96
$\frac{3}{4}$ x 2 x 2	$\frac{3}{4}$ x 2 x 2 in.	96.7	0.90
1 x 2 x 2	1 x 2 x 2 in.	128.2	0.86

*B_4C is 69.34 w/o B; B is 90.7 a/o B^{10}

d. EBR-II-type Radial Blanket Experiments; Radial Fission Rate Traverses. A number of experiments were run with various types of radial blankets containing depleted uranium designed to show the variation in U^{238} capture rate due to flux and spectral changes in the different blanket compositions. Radial traverses were first run at the reactor midplane with U^{235} and U^{238} fission counters through the regular radial blanket of 84 v/o depleted uranium and 9% steel. The depleted uranium blanket around 30° wedge sectors of both halves of the core was then replaced with an EBR-II-type blanket composition with about 42 v/o U^{238}, 30 v/o sodium, and 20 v/o steel. The substitution resulted in a reactivity loss of 22 Ih. Fission rate

traverses were then run through the blanket region with U^{235}, U^{238} and U^{234} fission counters, and a traverse was also made with a $B^{10}F_3$ proportional counter. The results indicated little change of the spectral character of the neutron flux in the EBR-II-type blanket region compared with that of the regular blanket.

Half the depleted uranium of the blanket of this EBR-II composition in the wedge sector was then replaced with graphite. The fission rate traverses and the BF_3 traverse were then repeated through the region. In this UC-type blanket, the neutron spectrum was appreciably softer, as would be expected, than in the EBR-II-type blanket. A general increase in U^{235} count rate of about 50% was obtained in the blanket, and the B^{10} reaction rate was about doubled.

A two-region radial blanket was next designed, with an inner radial zone of about 7-in. annular thickness and an outer zone of the same annular thickness, and constructed around the same 30° core sector. The inner radial zone contained the blanket of the EBR-II composition. In the outer zone, an EBR-II-type blanket was used, but with the depleted uranium replaced entirely by graphite, the resulting composition being 42 v/o C, 30 v/o sodium, and 20 v/o steel. Traverses through this blanket arrangement revealed only a small increase in the average fission rate for U^{235} in the inner EBR-II-type blanket zone from those rates found in the same region of the full EBR-II blanket. In the graphite zone, as expected, the U^{235} fission rate increased greatly (by a factor of three) over that in the outer region of the EBR-II type blanket.

Experiments are in progress in the blanket wedge sector reconstructed as the UC-type, with 21 v/o U^{238}, 21 v/o C, 30 v/o Na, and 20 v/o steel, determining the worth of enriched boron carbide columns in the blanket $\frac{1}{2}$ in. and 6 in. from the core radial edge. This is part of an evaluation of a rotary boron-carbide control rod system in this type of blanket. A similar experiment done in the normal 84 v/o depleted uranium radial blanket was described in the Progress Report, Oct 1962, ANL-6635, p. 11.

2. Preparations for ZPR-VI and ZPR-IX

a. Building 315. The air-conditioning system for the reactor cells has been tested and is satisfactory.

An extinguishing system which is to be available for combating uranium and other fires in emergencies is being installed.

Forty high-pressure storage tubes having a total capacity of approximately 1.7×10^6 liters of argon were placed on their foundations

on the west side of the building. The contractor is now in the process of installing the transmission piping from the storage tubes to the reactor cells.

A closure is being designed to cover the operating mechanisms on the emergency exit doors. This will prevent unauthorized tampering with the door operation.

b. ZPR-VI Assembly. The depleted uranium blanket material for the first core has been loaded into the reactor.

The dual-purpose rod drive mechanisms were connected to the control rod drawers and properly aligned.

During lifetime tests with a B^{10} insertion safety rod, it was found that there was considerable wear on the spring housing ring caused by contact with the moving spring coils. The aluminum spring housing on each drive will be replaced with one of stainless steel. This modification will not affect the startup of the facility, since these rods are to be used with large, dilute, fast core systems. These systems, however, are not scheduled for study for several more months.

c. ZPR-IX. The aluminum matrix tubes have been received. The Laboratory shops are reworking the tubes to meet dimensional specifications.

A vendor has submitted sample aluminum drawers for approval. Production of the drawers is expected to start immediately following Laboratory approval.

Checkout of the control console and interlock wiring is in progress. Some minor errors in wiring have been found and corrected.

d. Experimental Preparations. The Rossi-alpha time analyzer has been fabricated by the Electronics Division. It has been checked out with a thermal neutron source.

Calculations with the IBM-704 are being made to obtain the in-hours versus period relationship for the assemblies to be studied with ZPR-VI.

3. AFSR

a. Criticality Monitor. A criticality monitor, which would determine the degree of subcriticality of a shut-down reactor and be a highly desirable addition to the instrument panel of a reactor, has been under

development for the past six months. The machine has been assembled and is being tested in the beam hole of AFSR. During the past month, some preliminary data have been gathered which show the direction of future development and experimentation. Therefore, it seems appropriate at this stage to describe the device now in operation.

A schematic of the device is shown in Figure 2. With the reactor subcritical, a reciprocating oscillator worth about 0.1% $\Delta k/k$ modulates the flux at a low frequency (during current measurements, $\frac{5}{3}$ cps). The flux is detected by a sensitive, enriched BF_3 chamber, and the resulting signal amplified in a conventional linear current amplifier. A high-pass filter rejects the dc component, e_0, of the flux signal; the ac component is processed through a mechanically resonant filter which passes only the frequency of oscillation. The ac signal component is rectified ("detected") to yield a voltage representing the amplitude e_1. The dc and rectified ac signals are then processed by an analog divider which puts out a voltage proportional to e_1/e_0; this can be interpreted to give the amount of subcritical Δk if the worth of the oscillator is known. Figure 3 is a general photograph of the experimental set-up.

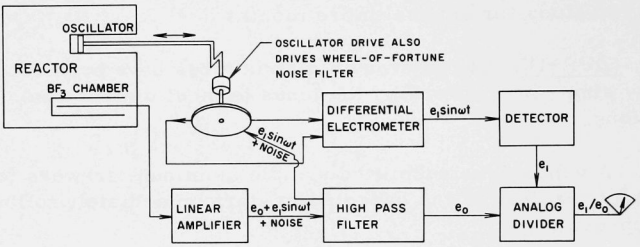

Figure 2. Experimental Criticality Monitor, AFSR

The "wheel-of-fortune" filter (see Figures 4 and 5) has worked very well. A wheel, carrying a capacitor array and commutator, is mounted directly on the drive shaft of the oscillator. Through the commutator the 36 capacitors are charged sequentially by the ac component of the neutron-flux signal. The charging time constant is such that the voltage existing at any one time on a given capacitor represents the average signal level of that portion of the cycle as obtained by averaging over a large number of cycles, and hence random noise or any frequency other than that at which the oscillator is being driven essentially cancels itself out. The voltage on the capacitor array is read out by a differential electrometer which has pickups 180° apart, thereby obtaining a signal twice the actual amplitude of the sine wave form impressed on the capacitors. The capacitance of the inputs to the electrometer are so low that the voltage of the capacitors on the wheel can be sampled many times without detriment to the voltage being "remembered" by the capacitors.

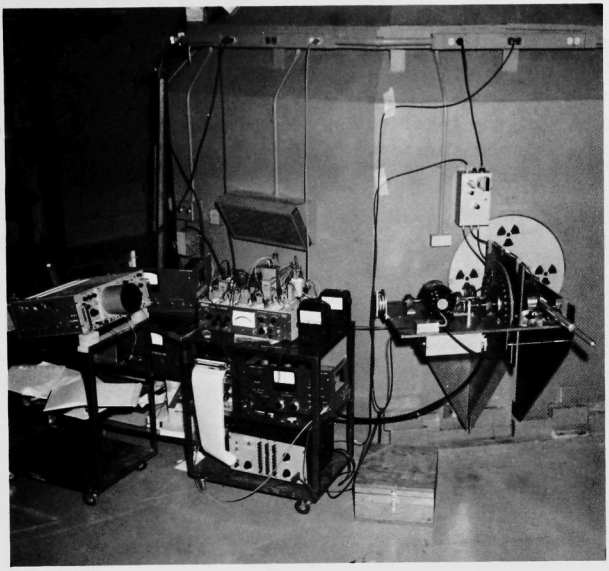

Figure 3. Experimental Arrangement for Test of Criticality Monitor at AFSR

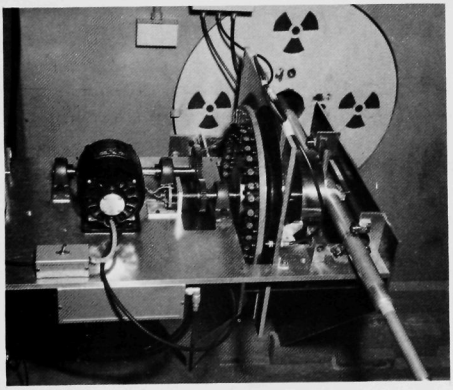

Figure 4. The "Wheel-of-fortune" Filter

It will be apparent that frequencies which are multiples of the base frequency will also be stored in phase; however, the RC inputs to the electrometer circuit are designed to suppress these harmonics. The effectiveness of the filter is illustrated in Figure 6; the resonance curves were obtained with the filter wheel driven nominally at $\frac{5}{3}$ revolution per second to examine the sine wave input from a Krohnhite oscillator at the frequencies indicated.

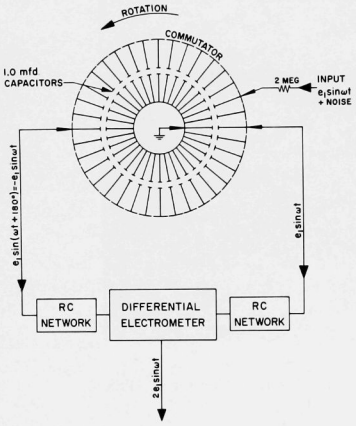

Figure 5. Wheel-of-fortune Noise Filter AFSR

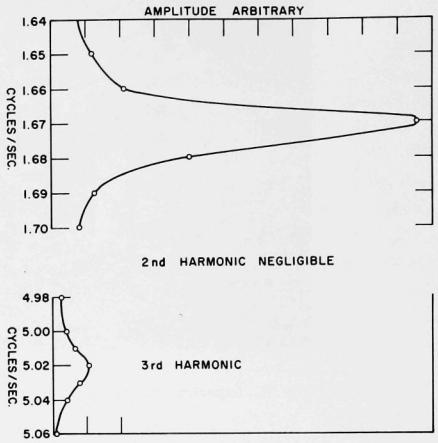

Figure 6. Filter Response at 5/3 Cycles/sec AFSR

The results of a few preliminary runs are shown in Figure 7. The line labelled "calculated" is that representing the predicted behavior from simple kinetic assumptions. The plotted points represent the meter readings of e_1/e_0 for two runs.

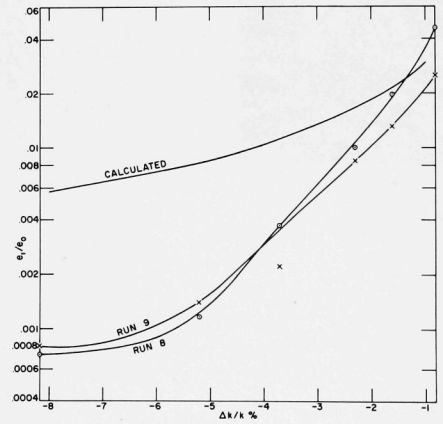

Figure 7

Criticality Meter Response e_1/e_0 vs $\Delta k/k$ AFSR

It is too early to draw any definite conclusions, but there are indications that:

1. The minimum acceptable signal from the chamber is of the order of 10^{-9} amp.

2. The time-response characteristics of the ac and dc branches of the circuit should be equalized; otherwise, the analog divider puts out wild information during changes in reactivity because one component responds more quickly than the other.

3. Considerable work is needed to shorten response time and improve sensitivity at lower reactivities.

Interlaboratory Comparison of Counting Techniques. An intercomparison of the counting techniques at three sites (Hanford, Los Alamos, and Argonne) for the determination of the number of fissions produced by irradiation of U^{235} and U^{238} showed good agreement in the values reported for samples subjected to identical irradiations (see Progress Report, Oct 1962, ANL-6635, p. 14). A similar procedure for non-fissile samples showed much poorer reproducibility of results. Samples of Co^{60}, Co^{58}, Sc^{46}, and Mn^{54} prepared by Hanford and measured by eight other sites yielded the preliminary results assembled in Table V.

Table V. Comparison of Results Counting Intercalibration Program

Site	$Co^{59}(n,\gamma)Co^{60}$	$Ni^{58}(n,p)Co^{58}$	$Ti^{46}(n,p)Sc^{46}$	$Fe^{54}(n,p)Mn^{54}$
A	1.06	1.04	0.58	1.14
	1.04	1.05	0.64	1.12
B	1.09	1.34	0.97	1.21
	1.02	1.25	1.20	0.91
C	1.06	1.26	1.27	1.23
	1.02	1.25	1.27	1.23
D	1.07	0.93	1.04	0.96
	1.02	0.94	0.98	0.88
E	1.00	1.64	1.31	1.58
	0.98	1.64	1.30	1.38
F	0.76	0.97	-	0.95
	0.74	0.97	0.94	0.93
G	1.00	1.24	1.27	1.22
	1.01	1.26	1.19	1.23
H	1.02	1.42	-	1.40
	1.04	1.43	1.34	1.43
Average	0.99	1.23	1.09	1.18
Standard Deviation	0.097	0.22	0.24	0.20

The values reported are ratios of the count rates determined by a particular group to those reported by Hanford. A meeting of the participants in this counting intercalibration program is being held at Argonne to attempt to determine the causes of the large discrepancies.

B. EBR-I

Unloading of the Mark III core in preparation for startup with the Mark IV plutonium loading was initiated on October 30 and was completed on November 8. All normal reactor instrumentation was in operation during the unloading procedure with the neutron source intact. The NaK coolant was circulated through the reactor and heated to 180°C before being transferred to the drain tank for precipitation of residual oxides.

Meanwhile, all Mark IV blanket rods were assembled with their extension handles in preparation for loading into the reactor. Since only 120 Mark IV blanket rods were available, they were arranged along the outer edges of the six subassemblies in the inner ring, 20 blanket rods per subassembly. The remainder of the positions in the inner ring of subassemblies were loaded with dummy fuel rods made of steel. The outer ring of blanket subassemblies remained, as planned, filled with Mark III blanket rods plus two instrument thimbles. The central subassembly was filled with fuel rods and readied for loading into the reactor.

During loading of the fuel for the approach to criticality, all normal reactor instrumentation was operating, and the reactor power-level safety circuits were limited to three decades above source level. The reactor flux level was recorded continuously. In addition to the normal instrumentation, five special counting channels were set up to monitor the approach to critical. Three were BF_3 counters, located in out-of-core vertical graphite holes, and two were specially made fission counters, about $\frac{3}{4}$-in. in diameter, in $\frac{15}{16}$-in. thimbles in the 12-subassembly ring of blanket, just outside the seven core subassemblies. These five counters were used to drive scalers, a log count rate meter circuit, and a linear count rate meter circuit. Counting rates were low on the in-core fission counters (loaded with 4 and 6 mg of U^{235}), and minor noise problems were particularly serious with these counting rates. However, satisfactory rates were obtained and loading was initiated.

The central fuel subassembly, containing 60 fuel rods (5.41 kg of Pu), was loaded into the reactor on November 20. Ten subsequent loadings - four of 42 rods, two of 24, two of 18, one of 8, and a final loading of 7 rods - brought the reactor to critical on November 27.

A typical curve of the inverse count rate obtained in the approach to critical is given in Figure 8. The loading at criticality, shown in Figure 9, consisted of 327 fuel rods containing 28.7 kg of Pu, with 27.1 kg of

Pu^{239}. The reactor was critical with the cup (outer blanket) at 1.0 in. below its uppermost position. Subsequent calibrations indicate that this last inch of motion is worth approximately 0.15% $\Delta k/k$.

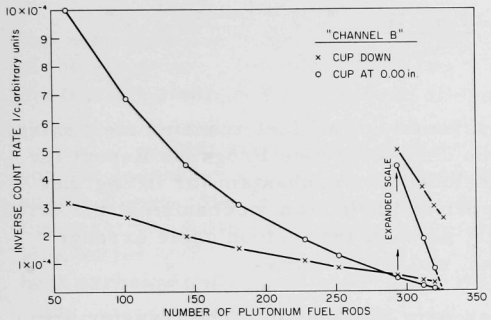

Figure 8

Inverse Count Rate for Approach to Criticality during Plutonium Loading

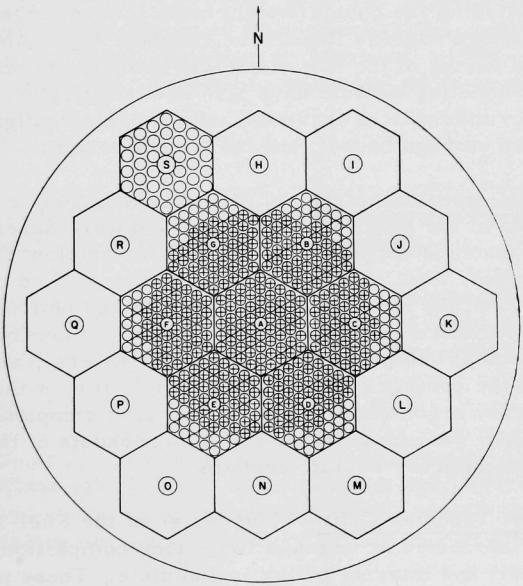

Fuel Rods - X
Blanket Rods - Blank

Figure 9. Final Loading of Approach to Critical EBR-I, Mark IV

Further determinations of cup worth, control and safety rod worth, the worth of fuel and blanket rods, and the worth of the two in-core fission counter thimbles are now being made.

C. EBR-II

1. Reactor Plant

a. Rotating Plug. The reassembly of all fuel-transfer mechanisms on the rotating shield plugs has been completed (see Progress Report for October, 1962, ANL-6635). This included the mechanism for lifting the reactor vessel cover, the fuel-gripper and holddown mechanisms, the drive motors for the rotating shield plugs, parts of the festoon cable arrangements, many electrical installations, and other items.

b. Modification of Transfer Arm Mechanism. The transfer arm mechanism, including the counterweight modifications, has been reinstalled in the reactor (see Progress Report for October, 1962, ANL-6635, p. 17). Installation and wiring of the new electrical components on the mechanism and to the fuel-handling console have also been completed. The unit was then checked for mechanical operation and properly realigned with the fuel gripper, the storage basket, and the transport port.

c. Fuel-unloading Machine. The following major components of this unit arrived at the EBR-II site in Idaho and were assembled on the fuel-unloading machine support rails in the reactor plant (see Progress Report for October, 1962, ANL-6635): the self-propelled carriage and platform structure, the shielded coffin, the gate and bottom seal ring, the moveable doughnut shield, the gripper drive, the control panel and electrical equipment cabinet, the sodium-vapor filters, the molecular sieves, and portions of the cooling systems. The installation of the previously shipped temporary argon cooling system was also completed. This work will be followed by various adjustments and checkouts of the mechanical, electrical, and temporary cooling systems.

d. Fuel Transfer Coffin. The design of the Fuel Transfer Coffin which is being fabricated at Argonne is nearing completion. Fabrication of the coffin shell and internal piping is complete. These parts are being assembled and the coffin is being prepared for filling with lead.

The heat-removal performance tests for the Interbuilding Coffin, conducted at the vendor's shops, indicated that approximately 4 kw of heat could be transferred to the coolant gas and subsequently removed from the gas by the heat exchanger. This heat-removal capacity is considered satisfactory. The major quantity of heat in the gas was removed in the internal annulus and only a small amount remained to be removed in the external air cooled heat exchanger. On the basis of these results, it was concluded

that the external heat exchanger and air blower were not required and could be removed. These modifications should not affect the heat-removal capacity of the coffin.

e. Primary System Components. The primary heat exchanger has been installed in the nozzle of the primary tank, and the installation of the secondary system piping between the primary heat exchanger and the flexible seals at the reactor plant containment shell is in progress.

Steel shielding balls were placed in the heat exchanger plug, and the secondary seal was installed between the heat exchanger and the nozzle flange. Welding of the 12-in. secondary piping and the 2-in. vent line was completed. The welds were radiographed, and the piping was leak tested with helium. A pneumatic pressure test of the piping and heat exchanger at 175 psig was successfully completed.

The primary sodium pump, M-2, was removed from its nozzle in order to permit access of personnel into the primary tank for final cleaning and for checkout of the fuel-handling system. Previously, the primary heat exchanger nozzle had been used as an access hole.

2. Power Plant

The gear train of the gear-motor-driven startup feedwater pump was disassembled in an effort to determine the cause of noisy operation. Reassembly must await instructions from the vendor.

The modification and repair of the cooling tower fan stacks were completed with the installation of new access doors. The top deck of the tower was reinforced with planking for greater structural strength.

3. Sodium Boiler Plant

The Package IV contractor has completed construction work in the Sodium Boiler Plant and checkout of the systems and components has been started. Checkout of the sump pumps, the cooling-water system, and the argon-supply system was completed.

Work was started on the following items: steam and water valve maintenance, drain valve checkout, Ansul system checkout, checkout of modified annunciator systems, testing of induction heating circuits, checkout of the cold trap Dowtherm cooling system, pipe location and movement checks, and thermocouple calibration.

4. Fuel Cycle Facility

a. Construction and Testing of Argon and Air Cells. The capacity of the shielding walls of the Air and Argon Cells for attenuation of gamma radiation was determined by employing radiation from three capsules of sodium-24 (each initially containing 1400 to 1800 curies) and surveying the exterior surfaces with scintillation instruments. About 11,000 sq ft of outside surface was covered, with the sources located on a 3-ft grid pattern adjacent to the walls, and at floor and ceiling positions of interest. Scanning was done both at points opposite the sources and at common grid corners, as well as at numerous specially suspect points.

The typical attenuation effected by the 5-ft, heavy concrete walls exceeded a factor of 10^8, and no evidence of major voids or leaks in the concrete was found. Somewhat smaller gamma attenuation was observed at spots near two Air Cell manipulator through-tubes, at the Air Cell door frame, in the vicinity of the sample-transfer port, and at the Argon Cell compressor feed-through. Minor corrective measures will be required at some of these points. Shielding limitations of the Argon Cell storage pits were also evaluated.

Preparations are being made to start leak testing of the Argon Cell. Initial tests will be carried out by reducing the internal pressure slightly and observing rate of pressure rise along with soap-bubble testing.

Leaks have been found in the welds on the bottom shield plug of the 7-ft-sq hatch in the roof of the Argon Cell. This hatch is to be used for emergency removal of equipment which is too large to be moved through the large transfer lock. Corrective measures to eliminate the leaks are being investigated.

The 400-cycle power system, painting and insulation, and piping to the Air Cell valve cabinets have been completed. Sleeves for the Model "A" manipulators were installed in Face 9 of the Argon Cell. Leak rating of the Argon Cell cooling boxes including Keystone valves and wiring to the Air Cell valve cabinets continued. Numerous leaks found in the leak check of the argon-distribution system are being repaired. The Kieley Mueller valves are being repaired and re-leak tested. The first valve repaired which had the largest leak on original test will not close (helium leak tight).

b. Testing and Development. System checkout and operability determination for one of the high-frequency in-cell furnace generator systems were carried out. When connected to one of the melt-refining furnace induction coils, output was somewhat less than expected. This will be further studied.

Exploratory tests have been made of the suitability of oil-impregnated sintered bronze sleeve bearings for use in high-intensity radiation areas of the Fuel Cycle Facility. The bearings tested were impregnated with either a commercially available SAE-10 oil or NRRO-358 radiation resistant oil (a product of Standard Oil Company of California). Dynamic tests were performed on nonirradiated and irradiated (to 1×10^9 rad) bearings using a load of 160 lb and a shaft speed of 310 rpm. Under these conditions the load was 50 percent of the manufacturer's maximum rating.

No significant improvement was noted in the performance of the oil-impregnated bearings over the performance of other bearings tested (see ANL-6287, p. 85). Further testing of the oil-impregnated bearings has therefore been discontinued.

Insulators molded from a Fiberglass-reinforced polyester compound are to replace the ceramic insulators presently being used for the crane bus bar collectors in the Air Cell. The greater impact strength of the Fiberglass plastic insulator was an important consideration in making this change. Test results of the physical and electrical properties of the plastic insulators after an exposure of 1×10^9 rad were considered satisfactory.

Distillation of magnesium-zinc in the melt-refining furnace is being studied as an alternative to retorting zinc-and-magnesium-coated uranium after the intermetallic decomposition step of the skull-reclamation process (see Progress Report, September 1962, ANL-6619, p. 21). A condenser design is being evaluated in which the condensed magnesium-zinc vapors are collected in a collector which will be discarded after each run. The condenser and furnace crucible, however, would be used for more than one run. The results of runs with collectors of four different shapes indicated that the shape of the bottom of the collector was important for the distillation of the final trace amounts of magnesium-zinc alloy from the furnace crucible and for preventing the formation of a magnesium-zinc bond between the collector and the furnace crucible, which would make their separation by remote handling difficult.

c. Development of Remote Control Methods and Equipment for Fuel Refabrication. Work has consisted mainly of (1) checking out and adjusting vendor-fabricated remotely controlled equipment for the EBR-II Fuel Refabrication, and (2) the design and construction of electrical controls for this equipment. The bonding machines, two settling machines, and a five-station leak detector were tested and shipped to the EBR-II site during the reporting period. Electrical controls for this equipment and for injection casting vacuum pressure systems were designed and constructed at ANL. These controls were tested and shipped to the EBR-II site.

The bonding machines and settling machines are similar in construction but different in size. The bonding machine shown in Figure 10 consists of a heating element over which is placed a cylindrical magazine containing 50 fuel rods for bonding. An insulating bell jar covers this magazine. The magazine of fuel rods is heated to 425°C; the fuel rods are impacted approximately 30 times per minute from the bottom through a series of driver pins. The impacts are supplied by a spring-mounted mass which is driven at resonating frequency by a solenoid. Because the resonating frequency changes slightly with the load on the machine, a pacer circuit was designed to synchronize the driving pulses with this varying resonant frequency. The units were designed for remote plug-in assembly. Figure 11 shows the solenoid driver unit supported by a manipulator tool.

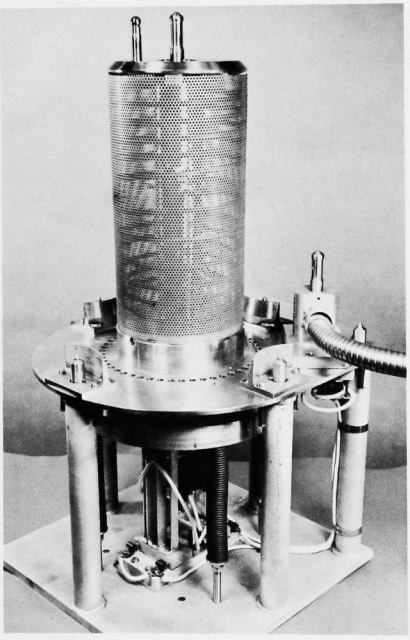

Figure 10

Bonding Machine without Magazine or Bell Jar Cover

The injection-casting furnaces and associated piping used for evacuation of the furnaces, pressurizing for casting, cooling, and circulating may be operated under a number of different conditions. In practice it has been found very difficult to be sure which section of pipe was at vacuum, at casting pressure, at cell atmospheric pressure, or containing cooling and circulating gas. In order to eliminate this confusion, a back-illuminated flow diagram was designed. This consists of a 19-in. square

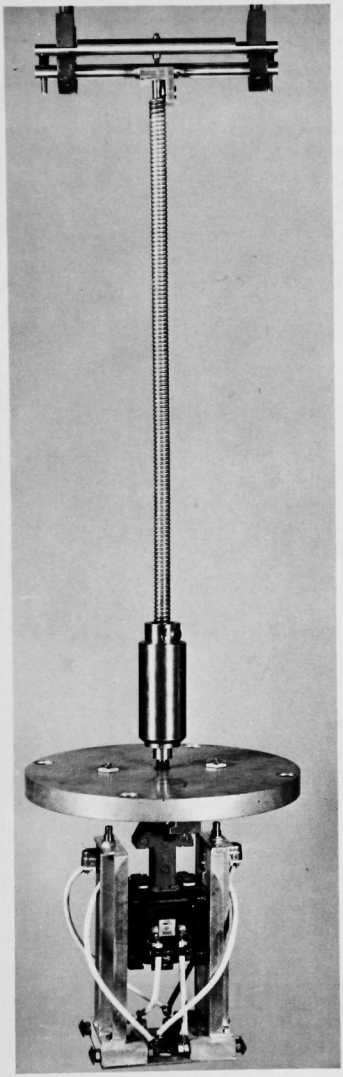

Figure 11. Plug-in Drive Solenoid Supported by Manipulator Tool.

lithographic negative sandwiched between sheets of clear Lucite. The pressure and flow conditions are indicated by 546 color-coded bulbs mounted behind this panel and wired to the sequencing controls of the injection casting furnaces to indicate the various conditions. The controls for the injection-casting vacuum pressure system and high-frequency heating are shown in Figure 12.

The testing, debugging, adjustment, and tuneup of the individual work stations on the pin-processing machine (see Figure 13) were started. Interchangeability of all the work stations and their subassemblies has been achieved. A number of corrective measures have been necessary to make this equipment work properly and to allow its remote disassembly and maintenance. It has been necessary to change the position of most of the manipulator pickup handles and lifting lugs to coincide with the center of gravity of each station. There were a number of inconsistencies found between the two machines and between the individual work stations for the machines and spare parts. These are being corrected to achieve true interchangeability. A number of instances of incorrect fit, improper lineup and poor workmanship are being corrected.

d. Installation of Fuel-fabrication Equipment. The dry argon-compressor system was leak detected; the control system was modified to effect the closing of the suction valves in the event of compressor shutdown, and time delay relays were installed in the low-oil-pressure circuit. The compressor startup was supervised by the representative of the Ingersoll-Rand Company. Objectionable leakage found in the distance piece covers was corrected. The Ingersoll-Rand Company representative also advised an increase in the size of the relief valve and piping from the first distance piece to the compressor suction.

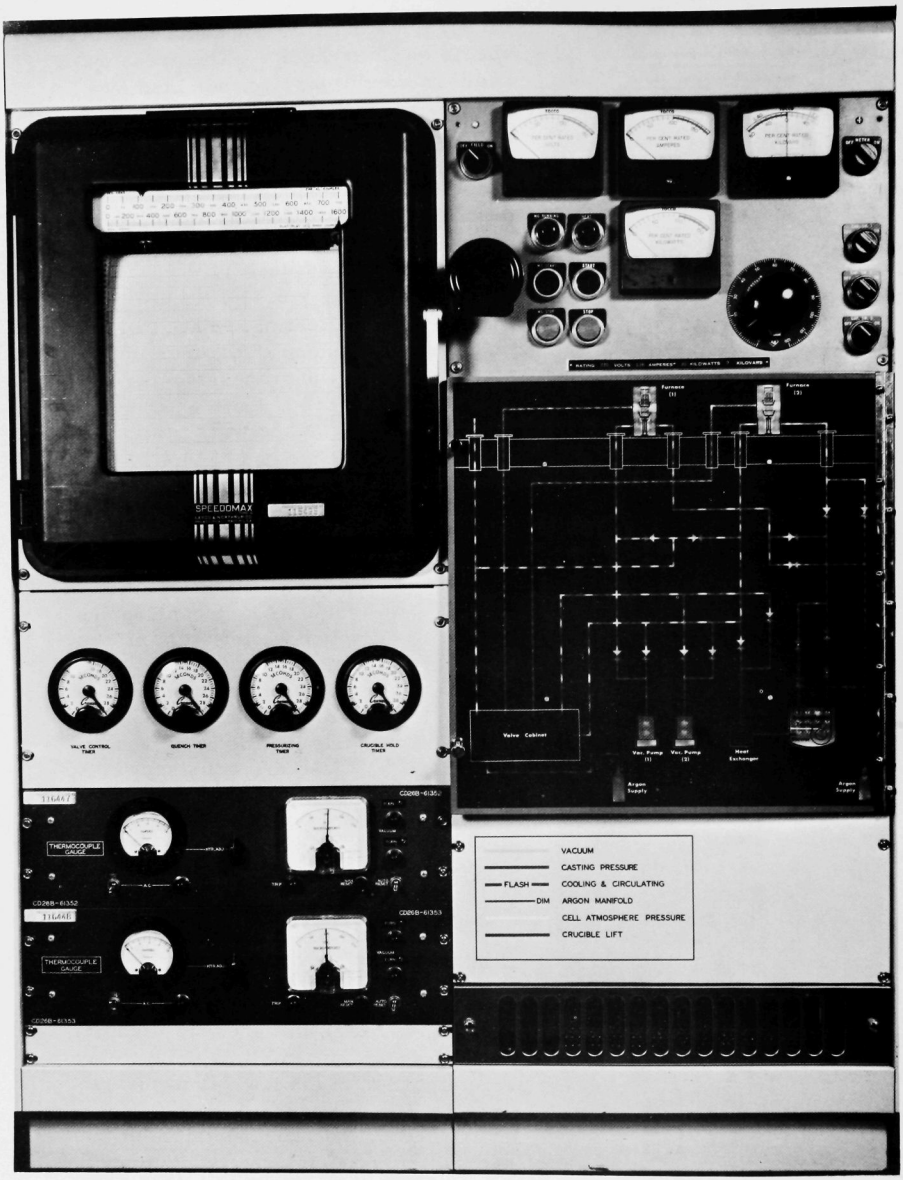

Figure 12. Controls for the Injection-casting Furnace and Vacuum Pressure System

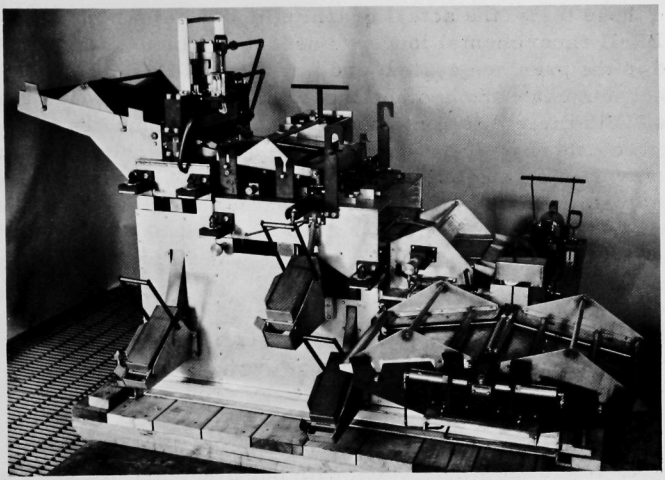

Figure 13. Fuel Pin Process and Inspection Machine

The fuel-element-assembly machine and the valve and relay cabinets were installed. Piping and mineral-insulated (MI) cable were extended from these cabinets through the shielded conduits of the Air Cell. Plug-in connectors were installed on the conduits within the Air Cell.

The 400-cycle power system has been installed except for final alignment of motors and generators. A thermocouple calibration furnace was assembled and wired to allow remote calibration of injection-casting furnace thermocouples.

e. Analytical Development. In the analytical laboratory, work on the lanthanum-139 method for burnup determination continued. Analysis of synthetic lanthanum mixtures (5-24 μg La^{139}) yielded results varying only 0.5-2.0 percent from the calculated values. In other samples simulating fissium alloy with 0.1-2.0 percent burnup, the deviation of results was 2 to 5 percent of the nominal values. A method for determining nitrides in fissium, which combines a Kjeldahl distillation with a colorimetric determination of ammonia, was tested with satisfactory results.

5. Development of EBR-II Fuel Element Monitor

A new test series for the EBR-II fuel-element-monitoring system, briefly described in ANL-6597 (Progress Report for July, 1962, p. 47), has been performed. Data from these measurements are still being processed.

In these tests, the actual graphite moderator which will be installed on the EBR-II experimental loop was used; this stack is somewhat smaller than used in the previous system and has a central cavity, 10 cm in diameter, to accommodate the coolant duct from the reactor. The tests were performed with three different neutron sources obtained by filling or emptying two concentric heavy water envelopes around the gamma source (a column containing a solution of irradiated NaCl). First, both envelopes were filled with D_2O and foils were irradiated for a flux plot; then, the inner envelope alone, which had a volume of about $\frac{1}{20}$ of the outer envelope, was filled; finally, the inner envelope alone was filled with heavy water diluted in the ratio of 1:10.

The flux plot, obtained with dysprosium foils, will be compared with a somewhat improved calculation of the neutron distribution in cylindrical geometry, using 16 neutron-energy groups.

In the course of these tests, it became evident that it will be necessary to shield the whole stack with boral against neutrons produced in surrounding concrete walls by photoneutron reactions.

A final checkout will be made after a shield has been added, after which the whole system will be ready for installation at the EBR-II. A comprehensive manual will be written to facilitate operation of the system by on-site personnel.

In order to obtain dynamic performance data, not available from the static tests which have been described, a smaller installation, which can be intercalibrated with the EBR-II system, is being designed to fit on the new TREAT sodium loop. The object of this work is to determine the extent and type of "signature" of actual fuel-element failures as an aid in interpreting the analogue signal from the system in terms of discriminating between actual failures and false alarms. Construction at the TREAT installation will start as soon as the more pressing work on the EBR-II system has been finished.

Work on improved fission chambers is meanwhile going forward; the second version of these chambers is now in the machine shop.

In the future, a new series of calculations is planned; these calculations will look into the possibility of improving the overall sensitivity of the system including the loading of fuel in the graphite stack to achieve a modest amount of neutron multiplication. The effect sought is a broadening of the thermal distribution, which would enable one to locate the detectors over larger radial distances from the source and thus decrease the gamma flux at the detector.

6. Fuel Development

a. Rate of Penetration of Cladding Materials by Molten Fuels.

Safety considerations for EBR-II require information about the rate of penetration of various prospective cladding materials by molten uranium and plutonium containing fuels. An apparatus for the testing of these materials up to 1500°C in a glovebox is now completed and checked out.

Type 304 stainless steel and Armco iron with molten uranium and uranium-5 w/o fissium were investigated using another apparatus (see Progress Report, April 1962, ANL-6565). An unpredicted, although reproducible, decrease in the rate of penetration of the iron and stainless steel with increasing temperature was found. To study this phenomenon further, the penetration rates of Armco iron by (1) molten uranium and (2) uranium-36 a/o iron eutectic (melting point 725°C) as a function of temperature have been determined.

Table VI contains all the data obtained with the present apparatus including some work that was done on uranium versus 304 stainless steel to check out the equipment. This table supersedes the previous data reported (see Progress Report, July 1962, ANL-6597, p. 20).

Table VI. Penetration of Armco Iron and Type 304 Stainless Steel by Molten Uranium and Uranium-36 a/o Iron Eutectic

Temp, °C	Molten Uranium						Molten Uranium-36 a/o Iron			
	Armco Iron				304 SS		Armco Iron			
	0.015 in.		0.030 in.		0.030 in.		0.015 in.		0.030 in.	
	Time, sec	Rate, mils/sec	Time, sec	Rate, mils/sec	Time, sec	Rate, mils/sec	Time, sec	Rate, mils/min	Time	Rate
740									49 hr	0.61 mil/hr
850									39 min	0.77 mil/min
950									10 min	3.0 mil/min
1050							84	11	3.6 min	8.3 mil/min
1070									3.3 min	9.1 mil/min
1085							0.6	25	1.4 sec	21 mil/sec
1138			0.9	33	1.3	23				
1150	0.5	30	1.1	27	1.3	23			1.1 sec	27 mil/sec
1169			1.1	27	4.3	7.0				
1187			1.3	23	7.3	4.1				
1206			4.4	6.8						
1229	3.1	4.8	5.7	5.3	7.0	4.3			3.7 sec	3.1 mil/sec
1244			5.2	5.8						
1300			3.7	8.1	4.6	6.5	1.7	8.8	4.4 sec	6.8 mil/sec

As can be seen by the data, the penetration rate of uranium-36 a/o iron through iron gradually increases between 740°C and 1070°C. When the temperature is increased to 1085°C, there is about a hundredfold increase in penetration rate above that found at 1070°C. The fact that there is a eutectic in this system that melts at 1080°C suggests that the rapid increase in penetration rate is caused by the formation of this eutectic. The rate then continues at about the same value to 1187°C, above which it decreases. Then again at 1244°C it begins to increase and continues to increase to 1300°C, our maximum test temperature.

In the range from 1150 to 1300°C the uranium (melting point 1132°C) vs iron data follow along well with the uranium-36 a/o iron (melting point 725°C) vs iron data. The rate of attack of Armco iron by uranium and by uranium-36 a/o iron is about the same. Superheat above the melting point of the molten material apparently has little to do with the penetration rate.

It should also be noted that the data indicate about the same penetration rate for 15-mil as for 30-mil test specimens. This would mean that the formation of an oxide or some other similar surface change is not responsible for the behavior observed.

We are continuing this study in an effort to understand the phenomenon better. The formation of an intermediate compound introduces more than one interface which must be considered in determining the rate-controlling process.

b. Fuel Jacket Development for Core II. Small quantities of Nb-1 w/o Zr tubing (the reference cladding material for Core II fuel) are being fabricated to the following sizes:

(a) 0.156 in. ID x 0.015 in. wall
(b) 0.156 in. ID x 0.025 in. wall
(c) 0.144 in. ID x 0.015 in. wall
(d) 0.144 in. ID x 0.025 in. wall

No apparent difficulties were encountered during the drawing operation. The tubes appear to be of good quality and are now ready for sizing and finishing stage operations.

The Nb-4 w/o V alloy bar stock of 0.450-in. diameter has been fabricated to 0.180-in. diameter for end plug stock for some of the Nb-4 w/o V tubing received from Westinghouse. The rods have been annealed and are being evaluated by hardness tests and metallographic examination.

c. Properties of Uranium-Plutonium-Fizzium.* Most of our metallurgical studies of uranium-plutonium-fizzium alloys as potential EBR-II fuels have involved the 20 w/o plutonium alloy. We are now examining alloys containing less than 20 w/o plutonium. Injection-cast rods of the following compositions:

U-10 w/o Pu	U-10 w/o Pu-10 w/o Fz
U-15 w/o Pu	U-15 w/o Pu-10 w/o Fz

have been made. Pertinent mechanical and physical properties of low plutonium-uranium fuels are being studied.

*The term "fizzium" has been adopted to denote a fissium composition with a higher than normal zirconium content.

d. Irradiation of Prototype Core II Fuel Rods. Postirradiation examinations are being conducted on a series of EBR-II Core II pins, fueled with U-20 w/o Pu-10 w/o Fs alloy and clad with refractory alloy tubing, which were irradiated in instrumented capsules in the CP-5 Reactor. The cross-sectional dimensions of the specimen duplicate the EBR-II fuel element. However, the length was reduced to a 2-in. fuel section and the void volume above the fuel was reduced proportionally.

The capsules were removed from the irradiation facility when it was evident that one or more of the claddings had failed. These failures were first detected by thermocouples and subsequently verified by either pinhole autoradiography or neutron radiography. Four unfailed specimens were punctured to determine the amount of fission gas release to the void space above the fuel.

The specimens were punctured in a 5-in.-long brass tube which was sealed at one end and had an O-ring coupling at the other. The coupling was attached to 15 ft of $\frac{3}{8}$-in.-diameter copper tubing leading outside the hot cell facility to a gas-collection system. The collecting and measuring system has been described previously.[3] The specimen cladding was pierced with a tool-steel needle which entered the side of the brass tube through a triple O-ring seal. A vacuum of 10^{-3} torr could be attained with a minimal static leak rate.

The volume of the combined piercing and collecting systems was 753 $\pm$ 26 cc. Pressure measurements were made with a 0-1 mm tilting McLeod gauge. The volume of released gas at STP was calculated from the pressure-volume relationship with an overall error no greater than $\pm$10%. The results are given in Table VII. An aliquot of the gas from each specimen was taken and has been submitted for mass-spectrometric analysis.

Table VII. Gas Release from U-20 w/o Pu-10 w/o Fs Specimens

Specimen No.	Maximum Cladding Surface Temp, °C	Burnup, a/o	Released Gas, cc at STP
CP-22-6	555	1.0	0.42
CP-23-2	535	1.4	0.16
CP-23-5	560	1.4	0.85
CP-23-6	560	1.4	0.65

Note: The irradiation specimen CP-22-6 differs in that the sodium bond between the fuel and the cladding had been purposely omitted.

[3] Annual Report for 1961, Metallurgy Division, ANL-6516, 147.

7. Process Development

a. Melt Refining Process Technology. Further evaluations have been made of the yield data obtained from the five small-scale, high-activity-level melt-refining experiments (see Progress Reports November 1960, February, March, and July, 1961, October 1962; ANL-6269, p. 31; ANL-6328, p. 37; ANL-6343, p. 41; ANL-6399, p. 31; ANL-6635, p. 22). In these experiments, approximately 400-g charges of 10 percent enriched uranium-five percent fissium pins, irradiated to burnups ranging from 0.22 to 1.75 total atom percent, were melt refined at 1400°C in lime-stabilized zirconia crucibles. In all instances the yields of purified metal in the product ingots were considerably lower than the yields obtained with unirradiated material in control experiments. To supplement yield data (yield values are ingot weights as percentages of charge weights), the weights of unoxidized uranium retained in the crucible skulls were determined for each of the melt-refining experiments. The total nonoxidized uranium was found to range from 91 to 96 w/o of the charge in the high-activity-level experiments and was 96 percent in a control experiment. However, only 57 to 78 w/o of the uranium metal appeared in the ingot in the high-activity-level experiments, whereas 90 percent of the uranium metal appeared in the ingot in the control experiment. The recovery of melt-refined metal by top pouring appears to be less efficient in experiments with irradiated alloys than in experiments with unirradiated alloys under the particular conditions employed in the small-scale, laboratory experiments. The reason for the difference in pouring yields is not yet known.

Two additional runs were performed in the investigation of the use of a chloride flux (calcium chloride containing magnesium fluoride as a rare earth oxidant) for melt refining under argon in beryllia crucibles (see Progress Report, October 1962, ANL-6635, p. 23). Each charge consisted of 700 g of uranium-5 percent fissium pins containing cerium (about 0.8 percent); the liquation temperature was 1200°C or 1100°C; and the liquation time was one hour. After removal of the salt phase by pouring and vaporization, ingots were poured at 1300°C. Yields were 97.6 and 97.4 percent, cerium removal was about 99 percent, and uranium loss to the flux was trivial (0.03 percent or less). No attack on a beryllia crucible was apparent after three runs. Although this procedure has utility for processing uranium fuels, application of this method to plutonium-containing fuels needs study. McKenzie and coworkers[4] have shown that plutonium is oxidized and lost to the flux when a magnesium chloride flux is used. The applicability of this process to plutonium-containing fuels will depend therefore upon the extent to which plutonium is lost to the flux when a small amount of oxidant is present in the flux.

Installation of equipment to be used in the study of iodine behavior during melt refining is nearly complete.

[4] D. E. McKenzie, W. L. Elsdon, and J. W. Fletcher, Can. J. Chem., 36, 1233 (1958).

b. Skull-reclamation Process. Construction of integrated equipment for large-scale (2.5 kg of skull oxide) demonstration of the skull-reclamation process is nearing completion. Equipment check-out should begin in December, and process operations in January.

Equipment is also being constructed for study of modifications of the skull-reclamation process, especially chemical decladding of fuel pins in fused salt and molten metal systems. The equipment includes salt-flux-purification equipment.

c. Blanket-processing Studies. A tenth run (4-kg uranium scale) was made to demonstrate phase separation in the blanket process. In this run, the magnesium-zinc-uranium charge was stirred at 800°C, magnesium was added to precipitate uranium, and the mixture was cooled to about 400°C prior to the removal of the supernatant phase. A 95 percent phase separation was achieved, which is considered satisfactory. The solidified uranium-magnesium-zinc heel remaining after phase separation was broken into small pieces satisfactorily. Breaking of heels will be necessary in both the skull-reclamation and blanket processes, since the heels will be transferred to smaller crucibles for retorting.

d. Materials and Equipment Evaluation. A study to determine the effect of flux and zinc-magnesium on the wettability and permeability of beryllium oxide was continued (see Progress Report, October 1962, ANL-6635, p. 24). Upon holding a 50 percent magnesium-zinc solution for 48 hr at 800°C in a thixotropically cast beryllium oxide crucible, some hairline cracks developed in the crucible. About 200 ppm of beryllium were introduced into the solution during the run. Despite the effects of the 48-hr run on the crucible, it was successfully used in short-term demonstration runs of the uranium precipitation and retorting steps of the skull-reclamation process under conditions similar to those in the 48-hr experiment.

Process vessels containing molten zinc may be housed in stainless steel equipment in order to control composition and pressure of the inert atmosphere. Since the stainless steel equipment may be exposed to zinc vapor, the corrosion resistance of various stainless steels to zinc vapor has been investigated. In 500-hr exposures to zinc vapor at 900°C, two austenitic 300 series stainless steels (Types 304 and 347) underwent severe attack. Superior resistance to attack by zinc vapor was exhibited by a 400 series stainless steel (Type 405, a ferritic steel). Another 400 series stainless steel, Type 440 C (martensitic), also exhibited fairly good corrosion resistance, although it suffered some loss in weight.

e. Removal of Nitrogen from Argon. Because it may be necessary to remove the nitrogen from the argon atmosphere in the Argon Cell of the EBR-II Fuel Cycle Facility, investigation of the kinetics of the reaction of nitrogen with titanium sponge has been started. Preliminary data indicate that the reaction of nitrogen with titanium sponge is controlled by diffusion of nitrogen in the solid titanium phase and that the reaction rate is very slow at the nitrogen concentrations of interest (100 to 5000 ppm).

8. Training

Twenty-eight technicians spent approximately 3,500 hr in training activities during the month. These activities included training in reactor technology, plant orientation, secondary sodium systems, health physics, and plant safety.

D. FARET

The structural material used in a fast reactor core can affect the physics safety parameters of the core considerably. For this reason computations are being made to determine the effect of different structural materials on the sodium void coefficient, fuel expansion coefficient, and the Doppler coefficient. In particular, it is of interest to find the physics effect as a function of the length-to-diameter (L/D) ratio for a given core. Preliminary results for one of the experiments contemplated for FARET, the 400-liter (medium-sized) core having volume fraction compositions of PuC-UC, Na, and Nb or stainless steel of 30, 52, and 18, respectively, are given in Table VIII. The computations indicate that the sodium void coefficient is more negative for the stainless steel structure than that of the niobium-structured core. The magnitude of this difference appears to be independent of the L/D ratio. The fuel expansion coefficient, on the other hand, is less negative for the stainless steel case. The difference is somewhat dependent on the L/D ratio.

Table VIII. Effect of Structural Materials in 400-liter Core on Coefficient for Sodium Voids and Fuel Expansion

L/D	Structure Materials	Plutonium Enrichment	Sodium Void Coefficient ($\times 10^6$)	Fuel Exp Coefficient ($\times 10^6$)
1.0	Nb	0.191	-1.0	-4.8
1.0	SS	0.173	-3.75	-4.3
0.5	Nb	0.197	-1.4	-3.16
0.5	SS	0.181	-4.53	-2.45
0.25	Nb	0.223	-2.75	-1.34
0.25	SS	0.211	-5.55	-0.55

III. GENERAL REACTOR TECHNOLOGY

A. Applied Reactor Physics

1. Measurement of Fast-Neutron Spectra

In ANL-6635 (Progress Report, October, 1962, p. 28) it was noted that significant improvement in the measurement of fast reactor spectra using a hydrogen-recoil proportional counter was limited by the gamma-ray intensity within a reactor. Tests have demonstrated that such measurements, however, should be feasible in fast critical assemblies.

In these tests, four standard ZPR-VI drawers were used to check the effect of surface background gamma radiation on a 5-cm-diameter recoil proportional counter filled with CH_4 at $\frac{1}{2}$ atm. Two drawers contained plates of enriched uranium (in addition to the depleted material), and the others contained only depleted uranium. Background electrons were present in the region of 5 to 100 kev, the range over which it would be most desirable to make measurements of neutron spectra by gaseous recoil techniques. Surface background from the bare depleted uranium was severe and was more than could be tolerated, but a 0.3-cm layer of lead around the detector sufficed to reduce the background to a very acceptable level. This quantity of lead should not create a level of perturbation beyond that already introduced by counter, preamp, cables, etc.

Various drawer-detector arrangements were checked for background, and it is concluded that, for new fuel, no difficulty beyond what can be handled by pulse-shape discrimination is to be expected. Gamma background in the region of measurement of neutron spectra will arise primarily from fission, and previous results obtained with a converter plate at ATSR indicate that gamma-initiated events will be about five times as frequent as proton recoils. This order of background is easily handled electronically.

Thus this technique for making spectral measurements is applicable for use in critical experiments in which the gamma background is due to a few watt-hours of energy release from new fuel but is not applicable where the background is due to fuel previously irradiated in an operating reactor having a history of more intense exposure.

Enough information is now available to permit making a very detailed account of the capabilities of gaseous total recoil devices for fast reactor spectroscopy, and it is hoped that this may be done at an early stage of ZPR-VI operation. Competition from other kinds of neutron spectrometers is not foreseen in the energy region below 1 Mev, nor is there much hope of using gas counters above about 1 Mev.

2. High-conversion Critical Experiment: ZPR-VII

Measurements continue to be made with a core assembly composed of 3 w/o enriched uranium, stainless steel-clad, Hi-C fuel pins in a 1.24-cm square pitch pattern, with emphasis on the accurate determination of reflector savings, neutron spectrum, and microscopic lattice parameters. Measurements related to control and safety have been concluded with a determination of the temperature coefficient of reactivity. For the range from 20 to 40°C an average value of -1.04×10^{-4} (% Δk)/°C was observed.

In order to minimize the error associated with the derivation of k_∞ from the Hi-C measurements, it is desirable that the buckling be determined with a high degree of precision. Because the height-to-diameter ratio is large in typical Hi-C cores, the radial buckling dominates over the axial component. Because of the small core radii, the region free from the influence of neutrons returned by the radial reflector is of limited size, so that radial flux patterns in particular must be measured quite accurately.

The adequacy of the conventional cosine and J_0 fits for the derivation of reflector savings from flux distributions is being investigated. A code has been written to determine axial bucklings of Hi-C cores. It is designed to do a least-squares fit for a number of flux traverses. Since some of the Hi-C cores are unreflected at the top, the usual symmetry considerations do not always apply. Thus the function to be fitted to each traverse was written as

$$\phi = C_1 \cos B_1 (x - x_0) + C_2 e^{B_2 x} + C_3 e^{-B_2 x} \quad ,$$

which is the most general solution of the two-group core equations in slab geometry. The results of two-group theory indicate that the bucklings B_1 and B_2 should be independent of neutron energy. Therefore, B_1 and B_2 were constrained to be the same for all traverses, while the other parameters (C_1, C_2, C_3, and x_0) could be different.

The code was tested for a set of eight patterns of axial flux, as determined with both bare and cadmium-covered 3% U^{235}, indium, dysprosium, and gold foils in a core containing a large central zone of 3 w/o enriched uranium, Hi-C fuel with a 1.13-cm triangular spacing. A total of 80 points was obtained, which, with 34 parameters, gave 46 degrees of freedom. The weights for the points were derived from the statistical errors calculated by the RE-202 foil data-processing code.

The value obtained for B_1 was 0.02292 ± 0.00026 cm^{-1}. The least-squares sum was 96.4, which is slightly over twice the number of degrees of freedom. This indicates that the discrepancies between the fitted function and the experimental points are outside statistics. This means that either the theoretical function is incorrect or that the errors on the points have been underestimated. If one adopts the latter interpretation, it implies

that the actual errors on the individual points are greater than the statistical errors by about a factor of 1.5, and that the error on B_1 should be multiplied by a similar factor.

A similar code for radial bucklings is being written.

3. Theoretical Physics

a. Scattering Law for Moderators. Two additions have been made to the Scattering Law data-processing computer program RE-216 to provide for results obtained from the Scattering Law for Moderators Experiment.

One of the additions is an interpolation routine, which finds for a predetermined fixed value of the energy transfer, β, the value of the Scattering Law $S(\alpha,\beta)$, and $S(\alpha,\beta)/\alpha$ as a function of α(the square of momentum transfer). For the given β and given incident energy, α is determined by the scattering angle. The procedure selects values of β close to the given value for each angle of scatter (as determined by the angular position of the counters). The corresponding values of $S(\alpha,\beta)$ are least-square fitted by a linear function, and from this fit the proper values of $S(\alpha,\beta)$ and $S(\alpha,\beta)/\alpha$ for the specified β are determined.

The second addition is a program to least-square fit $\log (S/\alpha)$ by functions $A\alpha^2 + B\alpha + C$ for small values of α. The limit as $\alpha \to 0$ of $\beta^2 \log (S/\alpha)$ is $p(\beta)$, which is the generalized frequency distribution. This is useful in deriving cross-section models[5] and in the extrapolation of the data.

b. Reactor Physics Data Analysis - ZPR-VII. Calculations of effective delayed-neutron fractions and prompt-neutron lifetimes have been made for the two BORAX-V uniform lattices and the Hi-C square and triangular lattices studied in ZPR-VII. Material constants for 15 fast groups and a thermal group were obtained by means of GAM-1 for the fast groups and of SOFOCATE along with disadvantage-factor calculations for the thermal group. The HOBO code was then used to obtain the fluxes and adjoints necessary for the calculations.

c. EBWR Plutonium Recycle Program. Physics calculations for the EBWR plutonium-recycle program are being performed. The loadings studied were of three different types; one-, two-, or three-zoned cores were studied, and the properties of each system were determined. The one-zoned core refers to an initially uniform core; the two-zoned core refers to a central 36-element plutonium region surrounded by a driver uranium region of a single enrichment; and the three-zoned core refers to a central 36-element plutonium region surrounded by a one-row region (28 elements) with uranium of one enrichment which, in turn, is surrounded by a uranium region of a second (lower) enrichment. The row surrounding the plutonium region may be referred to as the shim zone, and it is this row which will have its enrichment periodically increased in order to restore the reactivity of the overall system.

[5]Egelstaff and Schofield, Nuclear Science and Engineering, 12, 260 (1962)

Two designs of fuel elements were considered. One is the design of the EBWR Core 2 reference element, consisting of a 6 x 6-pin array of fuel tubes with an outer diameter of 1.07 cm. The other design consists of the same element and tube size except in a 5 x 5-pin array.

Various initial plutonium enrichments in the range from 0.5% to 5% were considered for the central region. The uranium region used the standard 6 x 6-pin array for all cases. The plutonium enrichment range of real interest is from 1.5% to 2.5%.

Initial reactivity coefficients and rod worths have been calculated for the various loadings that have been considered. Perhaps the most important conclusion from these calculations is that the void coefficient increases for systems with the higher plutonium enrichment. The increased void coefficient results in larger swings between the cold to hot voided conditions. Since the problem of control is very crucial in this loading, this factor argues quite strongly against a too-high plutonium enrichment.

Calculations have been made for the time behavior of reactivity and power distribution for the various loadings under what are believed to be realistic modes of operation. In the two-zone systems the reactivity is restored after each burnup step by reloading with a new enrichment. A burnup step was assumed to correspond roughly to 3000 Mwd/tonne in the central plutonium region. In the three-zone configuration only the shim row is replaced.

Although further calculations will be needed to specify precise properties, it is believed that sufficient calculations have been made to establish the following design criteria: (a) use the tube size and tube array of the reference design of Core 2; (b) the three-zone system; and (c) an initial plutonium enrichment of about $2\frac{1}{2}$% in the central region. The plutonium region would be surrounded by a uranium-fueled shim zone whose enrichment will vary as the experiment proceeds but may be expected to fall in the range of 2 to 5%. The outer region might well be natural uranium.

B. Reactor Fuel Development

1. Corrosion Studies

a. Niobium Alloys. Bend tests have been performed on the Nb-1.84 w/o Cr and Nb-4.33 w/o Zr alloys to determine if there was any ductility change accompanying the hardness change which resulted from the exposure to liquid sodium. The bend test consisted of loading the specimens in compression so that a free bend occurred. Compression was applied until the specimens fractured or a 180° bend was accomplished. Specimens with and without welds were tested. The specimens with welds were compressed with the weld in the direction of loading.

The welded, as-received, Nb-1.84 w/o Cr specimen cracked at the weld, but the parent material did not crack and was able to survive a 180° bend. Examination at 10x showed yielding of the material. In the

case of the sodium-tested sample, a crack initiated in the weld section (upon bending) and propagated across the entire sample. The specimen failed in a brittle manner. The as-received Nb-1.84 w/o Cr (without weld) survived a 180° bend. The sodium-tested sample fractured upon compression. The fracture was of a brittle nature.

The welded Nb-4.33 w/o Zr alloys exhibited the same behavior as the welded Nb-Cr samples in that the as-received specimen survived a 180° bend whereas the sodium-tested sample failed in a brittle manner upon application of compression. Both the as-received and sodium-tested Nb-Zr alloys (unwelded) failed, but the sodium-tested sample failed much sooner than the as-received sample.

Bend tests were also performed with as-received and sodium-tested Nb-5 w/o Mo specimens. Microhardness measurements across the transverse section of each of these samples showed the hardness to be constant, although the sodium-tested specimen was slightly softer. Both the samples survived a 180° bend without fracture.

As-received and sodium-tested samples of Nb-4.33 w/o Zr have been analyzed for oxygen, and the results (in ppm oxygen) are as follows:

	As-received	Sodium-tested
Analysis No. 1	60	1090
Analysis No. 2	76	1130

The oxygen concentrations reported are gross analyses of the specimens; probably the oxygen concentration at the edges of the sodium-tested sample are much higher than the reported figures indicate. It seems likely that the loss of ductility of the sodium-tested samples can be attributed to oxygen embrittlement.

b. Lightweight Alloy for Use with Mercury. As indicated in Progress Report, July 1962, ANL-6597, p. 31, nitrided commercially pure titanium was immune to liquid mercury during a 720-hr exposure in a quartz loop with a temperature differential of 96°C (from 275°C to 371°C).

A metal loop test of nitrided commercially pure titanium and three nitrided alloys: Ti-8 w/o Mn, Ti-2.5 w/o Al-16 w/o V, and Ti-7 w/o Al-12 w/o Zr, was conducted at higher temperatures. The loop is constructed of stainless steel Type 347 and is a thermal-convection type. An average flow rate of 19.4 ft/min and a temperature differential of 24°C (from 436 to 460°C) was maintained. After 984 hr of operation under these conditions, there was no detectable weight change for any of the samples, in either the hot or cold leg. Preliminary microscopic examination (at magnification 16x) of these specimens indicated no corrosive attack in either hot or cold leg. Metallographic examination of these specimens is under way.

c. Aluminum Powder Products. All the tubing types produced by Armour Research Foundation were removed from corrosion test last month after about nine months of exposure at 290°C. None of the samples was in satisfactory condition.

Direct extrusion tubing produced by Torrance Brass Company is still in test after about eight months. The French powder products which were added to the test about two months ago are in excellent condition.

d. Zirconium Alloys in Deoxygenated Steam. Long-term samples of Ni-Fe and Cu-Fe ternary alloys at 540°C and 600 psi (see Progress Report, July 1962, ANL-6597, p. 30) were removed from corrosion test after one month of additional exposure. Exposure times now range up to nearly 300 days. Those samples exposed for the longer times exhibit thick films which are cracked at sharp edges and generally are developing face film cracks as well. Weight change data have been obtained. Oxygen analyses and hardness tests will be made on a number of these specimens.

An experiment has been started to explore further the effect on corrosion samples of test procedure at startup and pretreatment in oxygen of the specimen surface.

e. Corrosion of Structural Materials in Superheated Steam. The past month has been devoted to the building and preliminary testing of a dynamic test facility. It has performed satisfactorily and a relatively long-time test is now being started in 100-, 200-, and 300-ft/sec steam at 650°C and 600 psig. Stainless steels 304 and 406 comprise the initial loading of samples.

2. Ceramic Fuels

a. Rare Earth Oxides. A study of the sintering of urania-ceria mixtures preliminary to the investigation of burnable poison additions to urania was undertaken. Compositions containing 0.5 w/o, 1.0 w/o and 3.0 w/o CeO_2 were compacted at pressures from 1.35 metric tons/cm^2 to 3.95 metric tons/cm^2 and sintered in hydrogen at temperatures from 1500°C to 1800°C for 4 hr. In comparing sintered data it appears that the ceria additions improve the sintering of the UO_2. Work is in progress to study the effect of an inert atmosphere on the sintering characteristics of the materials.

Compositions of 5 w/o Dy_2O_3-95 w/o UO_2 and 5 w/o Gd_2O_3-95 w/o UO_2 were compacted and sintered. From the physical data on the pellets there appears to be merit in broadening the scope of this investigation to study the characteristics of sintered compositions of dysprosia and gadolinia with urania for possible reactor fuels.

b. Plutonium and Plutonium-Uranium Ceramics. During the past year a major effort has been concentrated on the installation of gloveboxes and equipment in the new plutonium ceramics laboratory in Building 212. The first phase of construction has now been completed, although the present plans for this laboratory call for a gradual buildup of equipment over a period of several years. We are now conducting some preliminary studies

which are designed to give us more information about the sintering behavior and properties of plutonium monocarbide and other potential ceramic fuels which have a high plutonium density.

Buttons of PuC, Pu_3Si_2, PuSi, and Pu_xS_y were made by combining plutonium with the appropriate alloying elements in the arc furnace. Specimens for measurements of electrical resistivity were made by drop-casting several of these buttons into graphite molds so that they formed rods 1 in. long x 0.30 in. in diameter. The results of the resistivity measurements are given in Table IX, along with the values found by other investigators for similar uranium compounds. Arc-melted PuC has a resistivity value which compares favorably with the value of 230 microhm-cm for sintered material reported by Pascord. As with the carbide, Pu_3Si_2 had a resistivity value which was several times greater than the value obtained on U_3Si_2. This increase in resistivity for plutonium compounds may be an indication that the thermal conductivities of PuC and Pu_3Si_2 are less than the values found with equivalent uranium compounds.

Table IX. Resistivity Values for Some Plutonium and Uranium Compounds

Plutonium Compound	Resistivity, microhm-cm	Uranium Compound	Resistivity, microhm-cm
PuC	250	UC	41
Pu_3Si_2	215-250	U_3Si_2	80
PuSi	765-780	USi	-

Some of the PuC buttons which contained 46.5 a/o were used in sintering studies. Powder was made by pulverizing pieces of the arc-melted buttons to about -100 +325 mesh size. Dry pressing was attempted on the powder; however, the edges of the compacts crumbled during handling so a binder was added. The powder was coated with Carbowax 4000 or stearic acid and pressed in a die with a pressure of about 55,000 psi. These pellets were then repressed in an isostatic system at 60,000 psi in an attempt to get more uniform densification. The pellets were sintered under vacuum at 1435°C and 1535°C for 2 hr. The sintered densities are shown in Table X. Sintering was first attempted in a tantalum boat but there was a reaction of PuC with tantalum at about 1535°C. Therefore, a tungsten boat was substituted; no reaction was observed. Sintering at temperatures

Table X. Densities of Several PuC Pellets

Pellet No.	Binder	Green Density, g/cm³	% of Theory	Sintered Density (1435°C), g/cm³	% of Theory	Sintered Density (1535°C), g/cm³	% of Theory
1	Carbowax 4000 (1 w/o)	9.9	73.5	11.3	83.7	11.1	82.2
2	Carbowax 4000 (2 w/o)	10.5	78.0	11.8	87 4	12.0	88.8
3	Stearic Acid (1 w/o)	10.7	79.8	11.9	88.1	11.1	82.2

of 1500°C caused the pellets to assume a concave shape which was probably a result of a high forming pressure in the die. Future work will be directed toward obtaining higher green densities by means of the isostatic press, which should result in uniformly shaped pellets with densities above 90% theoretical.

c. Uranium Carbide. Preliminary investigations have been carried out on the preparation of uranium monocarbide by the reaction of a 23 weight percent uranium-zinc intermetallic compound with methane at 750° to 800°C. With this method, the zinc is expected to distill out, leaving a porous, low-density uranium structure that facilitates the reaction with methane. In each of three runs, the reaction rate appeared to be constant up to and beyond the point where one mole of methane reacted with one mole of uranium. A nonhomogeneous product was obtained. Additional studies of this reaction are being planned.

Work continued on the sintering of uranium monocarbide made by the precipitation technique and also of some carbides made by other methods. In Progress Report, July 1962, ANL-6597, p. 32, work was discussed in which shrinkage versus linearly rising temperature was determined in a vacuum dilatometer (1) for the precipitated carbide and (2) for some carbide made by the reaction of methane with hydrided uranium obtained from a commercial supplier. It was determined that shrinkage began very slowly at 750°C and gradually increased until at 1200-1300°C it was very rapid. Between 1300-1400°C the shrinkage began decreasing, and at 1450-1500°C it virtually stopped.

Similar shrinkage curves have been determined for uranium monocarbide made by arc melting and by the reaction of UO_2 and carbon. Each of the materials was milled to a range of particle sizes similar to those for the previously measured carbide powders. The procedures duplicated those previously done. The results showed that carbides made by these methods also sinter in the same temperature range. Sintering occurs between 800°C and 1500°C; above 1500°C, further densification is very slow.

On the basis of this work it is thought that uranium monocarbide can be sintered to greater than 90% of theoretical density at temperatures no greater than 1500°C provided the oxygen contamination is kept very low (i.e., $<0.2\%$) and powders are used with particle sizes less than 15μ. It is probable that sintering in a very clean argon atmosphere at a pressure of one atmosphere would be desirable, as the $UO_2 + UC$ reaction proceeds very slowly, if at all, at 1500°C at this pressure.

Specimens have been sintered to date to densities of 85-90% of theoretical density in vacuum, and all of these specimens were made from powders containing greater than 0.5% oxygen.

d. Uranium Phosphide. The objectives of this study of the UP system are to characterize the various compounds and to evaluate their potentials as reactor fuel materials. Compounds are currently being synthesized by solid-solid reaction of the elements, although other synthetic methods will be investigated.

Chemical analysis of UP clinker, made by the solid-solid reaction, showed an oxygen content of 1.25%, corresponding to an oxide (UO_2) content of about 12%. Metallographic examination of the samples revealed the presence of UO_2 as a second phase, confirming the results of X-ray diffraction. Small amounts of metallic uranium were also observed in some of the samples, also confirming results of X-ray diffraction. The UO_2 occurred as small stringers along the UP grain boundaries and were only occasionally surrounding the rounded UP grains.

The clinker exhibited a molten appearance microscopically, which is corroborated by the macroscopic appearance of the clinker, as well as observations on the temperatures attained during the highly exothermic U + P reaction. The microstructural characteristics of the UP clinker did not appear to have changed significantly as a result of arc melting, which would not be unexpected if the original clinker had been molten during formation.

UP has been made using uranium metal powder derived from forms of uranium other than chips. These UP and uranium powder samples are being analyzed for oxygen content in an effort to trace the source of oxygen contamination.

e. Uranium and Thorium Sulfides. A preparation process for uranium monosulfide utilizing uranium tetrafluoride as the starting material was continued. The sulfur source is a mixture of hydrogen sulfide and hydrogen gas. A molten chloride bath, composed of 50 m/o NaCl and 50 m/o KCl, was used to prevent the formation of hydrogen fluoride.

In an effort to minimize oxygen contamination, thereby decreasing the amount of UOS formed, hydrogen chloride gas was bubbled through the molten salt to remove occluded moisture. The equipment for this process is being reworked to accommodate the addition of the HCl gas and to provide a more impermeable reaction vessel.

Melting points were determined in hydrogen for a US-ThS solid solution series. The compositions had been vacuum sintered at 2000°C. The melting point dropped from 2450°C for US to about 2300°C for the 75 m/o ThS solid solution, then increased to 2335°C for ThS. It appeared that the ThOS phase, present up to 3 w/o in ThS, may have caused some lowering of the melting points of the solid solutions and ThS. Determinations run on different US batches, however, showed no depression of the melting point due to the presence of up to 3 w/o UOS.

US showed good compatibility with many metals which might be used as cladding, bonding, matrix, or thermocouple materials. The method used consisted of firing US pellets containing 25 v/o of metal filings for 2 hr at 1650, 1825 and 1980°C in vacuum.

Similar tests made with tantalum and vanadium in argon are described in Progress Report, August 1962, ANL-6610, p. 44. A combination of X-ray and metallographic analysis was used to determine whether reaction had taken place. Tantalum, molybdenum, vanadium, niobium, and W-26% Re showed no evidence of any reaction at all with US up to the maximum temperature of 1980°C. Vanadium did not react even as a liquid above its melting point of 1730°C.

Zirconium showed a severe reaction. At 1650°C, the main body of the pellet had a contracted US lattice parameter indicating that some of the zirconium had gone into solid solution. An unidentified phase had migrated to the surface of the pellet, forming a shell. At 1825°C, it appeared that all the zirconium was in solution and that liquid-phase sintering had taken place.

The room-temperature electrical resistivity was determined for three different solid solution series. Values of 200-300 $\mu\Omega$-cm for US and of 30-40 $\mu\Omega$-cm for ThS were obtained. The general pattern was for a resistivity increase from US to $U_{0.75}Th_{0.25}S$, then a steady decrease towards ThS. A US specimen showed an definite increase from 179 $\mu\Omega$-cm at 25°C to 181 $\mu\Omega$-cm at 50°C. A positive temperature dependency is typical of metallic conductance.

Using the Powell ball technique, Dr. McElroy at ORNL determined the thermal conductivity of a US specimen from ANL to be 0.0264 cal/cm-sec-°C at 75°C. This is about 35% higher than that determined for stoichiometric UO_2 in the same apparatus. Not enough work has yet been done to establish the temperature dependency, but it is expected that the conductivity will remain fairly constant with temperature. A ThS specimen has been prepared for the same apparatus.

Six specimens of uranium sulfide jacketed in 0.012-in.-thick Nb-1 w/o Zr alloy cladding with a 0.002-in. helium annulus are under irradiation in the MTR. The specimens are 0.281 in. in diameter and 3 in. in length. The fuel section is 2 in. long and each specimen contains a $\frac{1}{2}$-in.-long gas space above the fuel. The fuel is in the form of pressed and sintered pellets.

The specimens are being irradiated in stainless steel NaK capsules. The experiment is programmed to give cladding surface temperatures of 500, 600, and 800°C at cladding surface heat fluxes of 6.8×10^5, 9.3×10^5, and 11.5×10^5 BTU/hr-ft^2, respectively. The first specimens will be examined after approximately 1 a/o uranium burnup has been achieved.

3. The Thorium-Uranium-Plutonium System

The solid solubility of uranium and plutonium in thorium is being investigated as part of the study of the ternary system. Since the solid solubility of plutonium in thorium is large and that of uranium in thorium relatively small, isothermal sections through the thorium corner of the diagram should show the ternary field of solid solubility to be oblong and to run roughly parallel to the binary thorium-plutonium side. Thus, initially, one binary and two ternary series of alloys were prepared by arc melting from high-purity metals with a constant 0, 2, and 4% uranium and increasing amounts of 0, 10, 20, 30, 40, 50, and 60 w/o plutonium. The alloys were heat treated at 900 and 700°C for two days and five days, respectively, and water quenched.

The initial examination showed that, at 900°C, alloys with 0 and 2% uranium and with 40 w/o and more plutonium were partially melted. The same happened at 700°C to the binary alloys with 50 w/o plutonium and more. This is in agreement with the binary phase diagram by Poole, Williamson, and Marples,[6] according to which the solid solubilities at 900 and 700°C are 35 a/o (35.7 w/o) and 45.5 a/o (46.2 w/o), respectively. It also indicates disagreement with the Russian phase diagram,[7] in which the respective binary concentrations are 25.0 a/o (25.6 w/o) and 32.0 a/o (32.6 w/o).

High-purity binary thorium-plutonium alloys in the form of arc-melted buttons have been prepared for metallographic examination by a conventional hand-polishing technique. The alloys had practically no inclusions. The successful electrolytic etchant consisted of 32 parts of orthophosphoric acid, 9 parts of water, and 59 parts of ethoxy ethanol at a current density of 80 ma/cm^2.

Arc-melted, high-purity thorium-plutonium alloys oxidize upon storage in our nitrogen glovebox atmosphere. Alloys with up to 20 w/o plutonium show only a slight degree of discoloration after a couple of months, whereas the alloys with more plutonium oxidize more readily. The rate rises as the plutonium content increases and is high at 60 w/o plutonium.

The densities of three alloys as cast from commercial thorium, dingot uranium, and reactor grade plutonium are shown in Table XI. Figure 14 shows their relationship to those of the binary alloys.

[6] D. M. Poole, G. K. Williamson, and J. A. C. Marples, A Preliminary Investigation of the Plutonium-Thorium System, J. Inst. Met., 86 172 (1957/58).

[7] A. A. Bochvar, S. T. Konobeevsky, V. I. Kutaitsev, I. S. Menshikova, and N. T. Chebotarev, The Interaction between Plutonium and Other Metals in Connection with their Arrangement in Mendeleev's Period Table, Proc. Second United Nations Conf. on the Peaceful Uses of Atomic Energy, 6 184-193, Geneva (1958).

Table XI. Density of Arc-melted Thorium-Uranium-Plutonium Alloys

Number	Nominal Composition (w/o) Th	U	Pu	Density (g/cm^3)
B779F	80	10	10	12.366
B776G	75	5	20	12.394
B778B	60	20	20	13.410

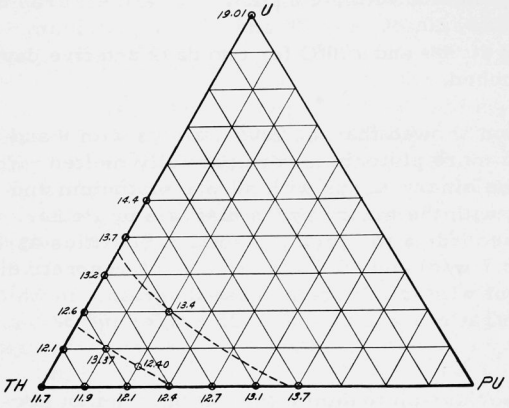

Figure 14
Density (g/cm^3) of Thorium-Uranium-Plutonium Alloys

Nondestructive Testing

a. Ultrasonic Imaging. One ultrasonic pickup tube, having a 5-Mc, 1-in.-diameter, quartz piezoelectric faceplate soldered to the glass frame of the tube has been successfully evacuated, processed, and sealed off. Life test studies are now in progress. The test seals made with epoxy techniques have all showed poor life properties. Future sealing efforts will be concentrated on improving the soldering seal methods. Parts for the assembly of a 2-in.-diameter pickup tube are now being collected.

b. Neutron Imaging. The intensities of thermal neutrons and gamma radiation in the neutron radiographic beam from the Juggernaut reactor have been measured for various thicknesses of lead and bismuth filters. Some improvement in the neutron-to-gamma ratio can be obtained by these filter techniques. Best results were obtained using bismuth filters of the order of 2 in. thick. The resultant decrease in neutron intensity, however, tended to offset the slight gains in neutron-to-gamma ratio, since the exposure times for direct exposure methods in the filtered beam tended to approach those required for transfer methods in the unfiltered beam. Nevertheless, these neutron-to-gamma ratio data

may prove useful in some application work. To complete this phase of the study, the intensities of thermal neutrons and gamma radiation were also determined as a function of reactor power. A linear relationship over a reactor power range of 100 times was obtained.

Technique curves for neutron radiographic inspection of uranium, lead, tungsten, and steel by several exposure methods are now in preparation. Some unusual aspects of the direct exposure curves for steel and tungsten, probably caused by prompt (n,γ) radiation from the inspection material, are now being more fully investigated.

c. Development of a Nondestructive Method for U^{235} Assay. A gamma scintillation spectrometry detector with a $\frac{1}{2}$-in.-diameter x $\frac{1}{2}$-in.-thick NaI crystal on a $\frac{3}{4}$-in. phototube was assembled for insertion into the CP-5 fuel tubes. This type of detector could be used for U^{235} assay without rotating the tubes. This would decrease the possibility of scratching the soft aluminum cladding, which has been a problem with handling the sample tubes on the lathe. The $\frac{1}{2}$-in. NaI crystal that was used is of poor quality and did not perform satisfactorily, but with a better crystal the I.D. probe may be a better approach than scanning the tubes from the outside.

d. Development of the Pulsed-field Reflection System. Development work has continued on the pulsed-field reflection system. This electromagnetic test method, with pulsed fields emanating from small apertures in special masks, replaces the sinusoidal currents and test coils or probes of our older eddy current test system. Test information about the metallic specimen being examined is received as a series of reflections from the surface and from inside the metal. This system represents a possible new approach to the problems of electromagnetic testing.

A 0.063-in. aperture had always been standard on mask-aperture assemblies used in this system, but tests on tubing of less than 0.020-in. wall thickness indicated that an aperture of 0.045 in. might provide a worthwhile increase in surface resolution and signal-to-noise ratio. The 0.045-in. aperture did provide a significant increase in resolution, but with a field loss of 20 db instead of the 8 db that had been expected. This loss has been traced to a defective pickup coil, and a new 0.045-in. mask-aperture assembly has been constructed to provide the improved resolution and expected field strength. It is now being compared with both the 0.063-in. mask-aperture assembly, and the dual-frequency sinusoidal equipment on the inspection of tubing; so far it has provided better performance than either.

At the same time, a 0.045-in. mask-aperture assembly of an entirely different type has been constructed. This provides a reflection signal at least 10 db higher than the type just discussed, but with some

loss in resolution due to a nonsymmetrical field near the aperture. It appears, though, that this loss is due to a fault in construction and not in its design. A new assembly of this type is being constructed.

5. Extrusion Development

A series of 12 copper billets were extruded on the 150-ton Lake Erie press to evaluate further the DPM (disposable particulate matter) tube-extrusion technique. Six 1-in.-diameter billets were drilled with a 0.656-in.-diameter hole while the remaining six billets were drilled with a 0.546-in.-diameter hole. Aluminum powder-filling techniques included -325 mesh powder poured in or compacted in the billet and -150 +200 mesh powder poured in. All billets were extruded at 725°C through a 0.359-in.-diameter radius entrance die (7.5:1 reduction ratio), with the exception of two large bore billets filled with compacted -325 mesh Al_2O_3 powder. These two billets were extruded at 725°C through a 0.344-in.-diameter die (8.2:1 reduction ratio) with a 120° included angle conical entrance. All billets extruded although two large bore billets fractured at the nose of the powder core.

Although evaluation is not complete, the billets loosely filled with -150 +200 mesh powder resulted in a more uniform wall thickness and concentricity than those filled with finer mesh powder. Billets with a smaller powder core appear to have a more uniform wall. The effect of compacting the -320 mesh powder seems to have little effect, but the compaction process only increased the packing density by about 5%.

The extrusions will be further evaluated and additional billets extruded.

Operational checkout work continued on the Lombard 350 ton vertical extrusion press with copper billets being extruded near the end of this reporting period. Although the extrusions were satisfactory, minor adjustments and modifications of the press are necessary, and further work will be done on the press prior to running ANL acceptance tests.

C. Reactor Materials Development

1. Radiation Damage in Steel

a. Dosimetry. The activation rates predicted by multigroup reactor calculations have been compared with foil measurements. The ratios are shown in Table XII for the four reactor locations being used in conjunction with irradiation of steel. The measured activation rate of sulfur was used for normalizing the calculations.

Table XII. Ratios of the Predicted and Measured Activation Rates of the Dosimeter Monitors

[Normalized to $S^{32}(n,p)P^{32}$]

	Ni^{58}	Fe^{54}	U^{238}
EBWR	0.95	0.90	1.25
CP-5 Fuel	1.0	1.18	0.594
CP-5 Dummy	0.815	1.5	0.233
EBR-I	1.0	0.94	-

The agreement of nickel and iron activations is adequate, with the largest discrepancies being for that carried out in the CP-5 dummy. This is probably due to the high thermal-to-fast flux ratio, which requires the use of chemical separation to determine the Mn^{54} activity. The errors inherent in this method have not yet been fully resolved. The rates of U^{238} fission checked poorly. This may be a result of fissions in U^{235} despite the use of 40-mil cadmium covers.

b. Relative Damage Rate Predictions. Based on the dosimetry results cited above, the energy-dependent model was used to calculate effective rates of irradiation damage produced in different facilities. Table XIII gives these relative rates, arbitrarily normalized to the dosimeter location in EBWR.

Table XIII. Relative Rates of Production of Damage by Irradiation

(Normalized to the Dosimetric Position in EBWR)

EBWR (20 Mw)		
Dosimeter	r = 85 cm	1.0
Vessel Wall	r = 106 cm	0.074
CP-5 (4.6 Mw)		
Fuel Element		147
Dummy		13.8
EBR-I (1.2 Mw)		
	r = 4.3 cm	86.6
	r = 7.6 cm	70.0

c. Irradiations and Mechanical Tests. All material irradiated in EBR-I has been returned to Argonne, Illinois. This includes Croloy ($2\frac{1}{4}$% chromium-1% molybdenum) impact and subsize tensile specimens, copper and silver single crystals, and some additional A-212B carbon steel impact specimens. These A-212B specimens have been broken and the data recorded.

The first set of A-212B impact specimens from EBWR, which received about 414 effective hours of exposure at 20 Mw, do not appear to indicate much of a shift in transition temperature. They were irradiated at about 305°C, which is the start of an annealing range, while the EBR-I specimens were held at 140°C. A shift of about 150°C was observed after 80-hr exposure in EBR-I at r = 4.3 cm.

The first of a series of specimens to be irradiated in CP-5 has been loaded. These specimens will receive from one to 30 days of exposure at a reactor power level of 4.6 Mw.

2. Fluid-control System for Water Reactors

A study on the feasibility of using fluid control systems in water reactors, using both neutron absorbing gas and liquid in tubes was completed last year. An experimental study is in progress and the necessary equipment is being assembled. A pressure vessel, valving, instrumentation, and associated piping is now being assembled and tested for use in the program.

D. Heat Engineering

1. Boiling Liquid Metal Studies

The construction of the working model of the electron-heated concentric tube test unit described in ANL-6619 (Monthly Progress Report for September, 1962, p. 45) is nearing completion. The model consists of a 0.020-in.-diameter, thoriated tungsten cathode fitted inside a $\frac{1}{2}$-in.-O.D., 0.35-in. wall thickness, Type 316 stainless steel tube (anode). This unit is one foot in length and the ends are closed with Kovar seals and water cooled. A vacuum in the tube is maintained with a diffusion pump. A power supply having a rating of 6000 v at 300 ma will be used in the initial studies.

The model will be used initially to make measurements of heat generation, cathode life with respect to pressure, anode voltage, and response to temperature control. The construction and operation of models with anode voltages up to 25,000 v and emission currents up to one ampere per square centimeter of cathode surface are contemplated.

2. Heat Transfer in Double-pipe Heat Exchangers

An analytical solution for the exchange of heat between two non-boiling, low Prandtl number fluids cocurrently (plug) flowing in infinitely wide parallel-plane channels and adjacent to a common wall was described in ANL-6635 (Monthly Progress Report for October, 1962, p. 41).

Recent work has been centered about three extensions of the analysis mentioned above as follows:

(1) Inclusion of the case in which the plug flow model for one of the fluids is replaced by the assumption of a uniform heat transfer coefficient. This case would be a fair approximation for heat exchange between the turbulent flow of a liquid metal and a fluid of relatively high Prandtl number, e.g., an organic coolant. An analytical solution for this case has been obtained.

(2) Use of the analyses for cocurrent plug flow as the basis for approximating results for a more realistic turbulent flow model. The study of this extension has introduced an interesting class of Sturm-Liouville problems with unusual boundary conditions. Further study is required before practicality of the analyses can be ascertained.

(3) Extension of the plug flow model to countercurrent flow. Solution of this problem has not been successful, and further investigations will be made.

E. Chemical Separations

1. Fluidization and Fluoride Volatility Separations Processes

a. Direct Fluorination of Uranium Dioxide Fuel. Engineering-scale studies have continued on the development of a two-zone oxidation-fluorination scheme for the conversion of uranium dioxide pellets into uranium hexafluoride in a single reactor. In this method, U_3O_8 fines are formed in the lower reaction zone by contacting the uranium dioxide pellets with an oxygen-nitrogen mixture, elutriated from the pellet bed, and fluorinated with fluorine in the upper reaction zone. Alumina is present in both zones as a fluidizing medium.

Another batch fluorination run has been made in the pilot plant to test the temperature-gradient method for improving operation in the lower oxidation reaction zone (see Progress Report, October 1962, ANL-6635, p. 44). In this run, the temperature at the top of the uranium dioxide pellet zone was maintained at about 400°C, and decreased to about 140°C toward the bottom of the zone. The upper fluorination reaction zone was maintained at 525°C. No difficulties with caking or with elutriation were encountered in this run which used a 12-in.-deep (8.8 kg uranium dioxide) static pellet bed and a 24-in.-deep fluidized alumina zone above the pellet charge. The weight of alumina charged was nearly equal to the weight of the uranium dioxide pellets. In the oxidation zone, the fluidizing gas, composed of 26 percent oxygen in nitrogen, was passed through the pellets at a total gas flow rate of 1.2 cfm. In the fluorination zone, the fluorine concentration in the fluorinating gas varied from 8.5 to 11 percent. The uranium dioxide charge was completely fluorinated in 17 hr with an

overall fluorine efficiency of 50 percent. Only about 0.05 w/o of the uranium initially charged was retained on the inert solid. Rates of uranium hexafluoride production were about 40 lb UF_6/(hr)(sq ft reactor cross section) and were similar to those reported previously (see ANL-6635, p. 45). During the initial one-third of the run, a fluorine efficiency (no gas recycle) of nearly 80 percent was achieved by basing the fluorine input to the reactor on the rate of uranium hexafluoride collection. Thus, high fluorine efficiencies appear possible with once-through gas flow. The run was satisfactory operationally; there were no difficulties with caking or with elutriation of the fines from the pellet bed.

b. Fluorination of Nickel-Thoria Alloy. A recent, commercially developed nickel alloy, having a composition of 98 percent nickel-2 percent thoria, was tested for its suitability as a material of construction for the containment of fluorine at elevated temperatures. Samples of the nickel-thoria alloy and of A-nickel were fluorinated in a static system at 600°C for 4 days. The data show that the nickel-thoria alloy reacts about an order of magnitude more rapidly than does the A-nickel. It has been concluded therefore that the nickel-thoria alloy would not be suitable for use as a material of construction in the application described above.

Separation of Uranium from Zirconium-alloy Fuels; Studies of the Chlorination and Fluorination Steps. Current bench-scale fluid-bed studies of the chlorination-fluorination scheme for reprocessing highly enriched uranium-zirconium alloy fuels are concerned with the evaluation of the effect that the use of separate streams of hydrogen and chlorine may have on uranium recovery. The use of separate hydrogen and chlorine streams is being considered as a means of providing make-up hydrogen chloride should gas recycle be used during the hydrochlorination step. Equipment modifications are underway and include the installation of an auxiliary combustion chamber in which the hydrogen and chlorine will be combined prior to their introduction to the fluid-bed reactor. By this procedure the presence of unreacted chlorine in the reactor will be avoided (the use of 20 percent excess hydrogen is planned), and uranium losses should be minimized by the formation of more volatile chlorides (compounds with a higher ratio of chlorine to uranium) during the reaction with the alloy fuel.

c. Fluid-bed Hydrolysis of Zirconium Tetrachloride. Investigation of the fluid-bed hydrolysis (by steam) of zirconium tetrachloride to zirconium dioxide was continued. Further studies were made of the use of sand as a starting bed material and the effect on operating conditions of a feed gas stream containing a high concentration of hydrogen chloride (about 60 volume percent) in nitrogen. The high concentration of hydrogen chloride in the feed stream more nearly simulates conditions proposed for the pilot plant (see Progress Report, October 1962, ANL-6635, p. 46). A 1:7:12 mole ratio of a mixture of zirconium tetrachloride, nitrogen, and hydrogen

chloride was used in the feed stream to the reactor. A run of $11\frac{1}{2}$-hr duration was made at an average zirconium tetrachloride feed rate of 2.6 kg/hr and with a quantity of steam equivalent to about 3.2 times the stoichiometric requirement.* The temperature of the sand bed was 350°C, and the initial bed weight was 20 kg. Operation of the column was considered satisfactory in that good temperature control was maintained in the bed (an indication of good fluidization) and pressure buildup did not occur across the sintered metal filters.

d. Conversion of Uranium Hexafluoride to Uranium Dioxide: Preparation of High-density Particles. Development continued on a fluid-bed method for preparing high-density spheroidal uranium dioxide particles directly from uranium hexafluoride by the simultaneous reaction of the hexafluoride with steam and hydrogen at temperatures in the range from 650 to 700°C. The feasibility of preparing uranium dioxide particles of a relatively coarse size (14 mesh and larger) is being investigated, since such particles are desirable for use in vibratory-compacted or dispersion-type fuel elements (see Progress Report, October 1962, ANL-6635, p. 46). Because of the high density and large particle size, gas velocities required to fluidize these particles cannot be accommodated by the present installation. Therefore, work has been started on a method in which a gas impulse is superimposed on the inlet gas flow to achieve improved mixing conditions in the reactor. Studies are underway to determine the pulse frequency, the total gas flow requirements, and the inlet hexafluoride nozzle position for optimum column operation.

2. Chemical-Metallurgical Process Studies

a. Chemistry of Liquid Metals. The solubilities of zirconium in a nominal 10 w/o magnesium-zinc solution were found to range from 2.7 w/o at 750°C to 0.1 w/o at 580°C. In a nominal 40 w/o magnesium-zinc solution, solubilities ranged from 0.9 w/o at 760°C to 0.06 w/o at 510°C. These may be compared with values obtained in 20, 30, and 50 w/o magnesium-zinc solutions (reported in Progress Report, July 1962, ANL-6597, p. 44).

Analysis of the solubility data for uranium in magnesium-zinc solutions in the composition range where metallic uranium is the solid phase indicates that the temperature coefficient of the solubility varies from very low values at 15.6 percent magnesium to moderately large values at 67.6 percent magnesium. At 800°C (the temperature at which uranium is dissolved in magnesium-zinc in one step of the proposed skull-reclamation process for EBR-II fuel recovery), the solubility of uranium varies from 12 percent in 15.6 percent magnesium-zinc solutions to 0.12 percent in 67.6 percent magnesium-zinc solutions.

---

*Based on the reaction: $ZrCl_4 + 2H_2O \rightarrow ZrO_2 + 4HCl$.

Emf data for the sixth galvanic cell in the series, $Pu/PuCl_3$, LiCl-KCl (eutectic)/Pu-Zn (two-phase alloy), have been obtained in a new cell over the temperature range from 466° to 670°C. This cell was similar in construction and operation to the fifth cell (see Progress Report, September 1962, ANL-6619, p. 51). The emf values can be represented by the equation

$$E\ (v) = 1.076 - 6.5_0 \times 10^{-4}\ T$$

with an average deviation of 2 mv.

Stoichiometry of the intermediate phases in the systems of zinc with lanthanum, cerium, praseodymium, and neodymium is summarized in Table XIV. A total of eleven crystallographically distinct phase types appear in these systems.

Table XIV. Intermetallic Phases in the Zinc Systems of Lanthanum, Cerium, Praseodymium, and Neodymium at 520°C

Lanthanum	Cerium	Praseodymium	Neodymium
$LaZn_{13}$	-	-	-
$LaZn_{11}$	$CeZn_{11}$	$PrZn_{11}$	$NdZn_{11}$
$LaZn_{8.5}$	$CeZn_{8.5}$	$PrZn_{8.5}$	$NdZn_{8.5}$
$LaZn_{7.25}$	$CeZn_7$	$PrZn_7$	$NdZn_{6.5}$
$LaZn_{5.25}$	$CeZn_{5.25}$	$PrZn_{5.25}$	-
-	$CeZn_{4.4}$	$PrZn_{4.3}$	$NdZn_{4.3}$
$LaZn_4$	-	-	-
-	$CeZn_{3.6}$	$PrZn_{3.6}$	$NdZn_{3.5}$
-	$CeZn_3$	$PrZn_3$	$NdZn_3$
$LaZn_2$	$CeZn_2$	$PrZn_2$	$NdZn_2$
LaZn	CeZn	PrZn	NdZn

In a continuation of the study of the technetium-zinc system (see Progress Report, June 1962, ANL-6580, p. 45), approximate compositions of two intermetallic compounds have been found to be $TcZn_6$ and $TcZn_{15}$. These compounds have not yet been completely characterized.

b. Liquid Metal Distillation. Rapid nonturbulent vaporization (see Progress Report, August 1962, ANL-6610, p. 59) of mercury was effected by the use of inductive heating and mixing. A vaporization rate of 800 lb Hg/hr/sq ft surface was achieved at a pressure of 1 to 10 mm Hg.

c. Reduction of Thorium Dioxide. Additional laboratory-scale (7 to 70 g of thorium dioxide) experiments have been performed on the reduction of thorium dioxide to the metal by zinc-magnesium solution in the presence of a halide flux. The effects of the following variables have been investigated: (1) rate of agitation of the flux-metal system, (2) the use of calcined thorium dioxide (prepared by heating thorium oxalate to 1000°C) as compared with the use of uncalcined thorium dioxide (prepared by heating thorium oxalate to 350°C), (3) the flux composition, (4) magnesium concentration in the metal phase, and (5) the ratio of flux weight to zinc-magnesium weight.

The solubility of thorium metal in zinc-magnesium solutions was also determined in the composition range of interest. The results were as follows:

(1) The rate of reduction increased as the mixing rate of the metal and flux was increased from 200 rpm to a maximum of 1000 rpm.

(2) No significant difference was found in the overall rates of reduction of calcined thorium dioxide and uncalcined thorium dioxide.

(3) By the use of a flux containing 47.5 to 50 m/o magnesium chloride, 10 m/o calcium fluoride and the remainder calcium chloride, complete reduction of a thorium oxide charge which yielded a thorium metal concentration of 9.1 w/o in the final zinc-magnesium solution was achieved.

(4) On varying the magnesium concentration in the metal phase, a marked maximum in the reduction rate of thorium dioxide occurred at 5 to 10 w/o magnesium.

(5) Variations in the quantity of flux used had only a small effect on the reduction rate of a given quantity of thorium dioxide by a given quantity of magnesium-zinc, although it is suspected that the rate would drop sharply beyond a critical amount of flux.

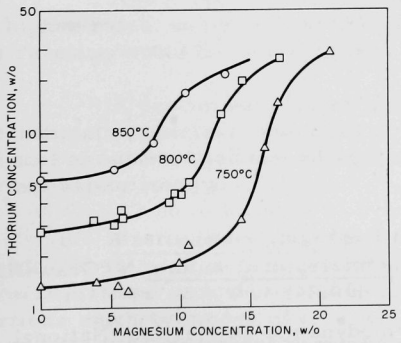

15. Solubility of Thorium in Zinc-Magnesium Solutions

The solubility of thorium in zinc-magnesium solutions was determined within the temperature and composition regions of process interest (see Figure 15). The solubility increases by a factor of about two for a 50-degree temperature increase in the range from 750 to 850°C. The thorium solubility also increases markedly with increasing magnesium concentration in the region of 5 to 15 w/o, depending on the temperature.

3. Calorimetry

The value determined for the enthalpy of formation of crystalline

uranium hexafluoride is $-522.8_7 \pm 0.4_8$ kcal/mole. This may be compared with previous estimates of -517 ± 3 kcal/mole reported by Katz and Rabinowich[8] and listed in the NBS Circular 500.[9]

A series of combustions to determine the heat of formation of ruthenium pentafluoride has been completed. Preliminary calculations indicate that the value for the net energy evolved per gram of ruthenium burned is approximately 2098 cal/g.

Techniques for the combustion of zinc in fluorine have been developed, and a series of combustions is in progress. An initial series of combustions of tantalum in fluorine has been completed, and calculations are currently in progress.

Experimental work on the determination of the heat of formation of zirconium diboride has been completed. Calculations are in progress.

---

[8]J. Katz and E. Rabinowich, The Chemistry of Uranium, McGraw-Hill Book Co., Inc., New York (1951), p. 412.

[9]Selected Values of Chemical Thermodynamic Properties, National Bureau of Standards Circular 500, U. S. Govt. Printing Office, Washington, D. C. (1952), p. 359.

IV. ADVANCED SYSTEMS RESEARCH AND DEVELOPMENT

A. Argonne Advanced Research Reactor (AARR)

1. Design

The drawings for the core supports, core, reflector, and control and safety rod mechanisms have been completed and authorized for construction. Preliminary estimates for the fuel costs have been obtained for sandwich plates containing the fissile material in the form of highly enriched uranium foil covered with stainless steel sheet.

An examination has been made of the relative merits of resistance welding of the fuel sandwiches as against bonding with plastic. A tentative decision has been made to use the resistance welding method for fabricating the AARR critical fuel.

A set of compact rod drive mechanisms have been tested for reliability. A supplementary coarse-position indicator for the new rod drives is now in the construction stage.

2. Research and Development

a. Critical Experiment. The critical properties for a variety of critical arrays have been established. Control by B^{10} poison requires a maximum of one B^{10} atom per 13 U^{235} atoms.

Transient studies show that the core will withstand the effects of step insertions of reactivity up to \$1.50 before any fuel melts. The Doppler coefficient provides a prompt negative coefficient of limited size ($<30¢$) which, however, is effective only in very sharp transients.

Ramp reactivity insertions up to $30¢/sec$ are self-regulating. At higher rates, unstable bulk boiling will occur (after many seconds) and the reaction would be self-limiting.

A preliminary hazards memorandum covering the essential mechanical, electrical, operational, and nuclear features of the proposed critical assembly has been written as a preliminary step in initiating the formal safety review.

b. Preliminary Hazards Analysis. The results of studies show the AARR (50-30) core to be inherently self-limiting with respect to short-term transients such that safe conditions are maintained for reactivity insertions much in excess of expected maximum accidental reactivity disturbances. Long-term responses to severe reactivity insertions will require corrective action through the control and/or safety systems to

maintain core safety. However, the long-term approach to dangerous conditions is sufficiently slow that the control system response requirements are quite modest.

Some details of the hazards analysis show:

Site Studies. The argon-41 dose rate produced in surrounding areas by normal discharge from the AARR exhaust stack has been calculated and found to provide negligible background in the neighborhood of low-level counting rooms. Estimated concentrations are 10^{-16} c/liter for a 250-ft stack and 10^{-14} c/liter for a 150-ft stack.

Analog Computer Core Dynamics Study. The inherent dynamic response of the AARR core having 0.050-in.-thick fuel plates and 0.030-in. coolant channels to various reactivity disturbances has been studied assuming an appropriate theoretical model and analog computer program. The model used is similar to the one used at Brookhaven to study the transient behavior of HFBR and has yielded results which are in good agreement with measurements made in SPERT-III tests.[10] Some modifications to the Brookhaven model were made where necessary or desirable to facilitate its application to the AARR case. Major features of the model are:

(1) Kinetics - Conventional, point reactor, neutron kinetics equations are employed.

(2) Heat Transfer - The core is considered to be divided into four axial segments chosen such that each segment contains equal amounts of power. The equations yield the average temperatures in the fuel, clad, and associated water for each axial segment of an average(i.e., one generating average power) fuel plate. Temperatures at other locations in the core are related to those associated with the average fuel plates through the power density distribution function.

(3) Steam Generation - Incipient boiling is assumed to occur when clad temperature exceeds saturation temperature. Then a fraction of the total power generated is assumed to be utilized in the generation of steam which is transported at water velocity through the core. Collapse of steam bubbles is neglected.

(4) Compensated Reactivity - The primary inherent reactivity-feedback effects are considered to be those which cause water voids. In addition, a reactivity term due to spectrum shift with water temperature is included. The factors effecting the feedback reactivity are evaluated through the use of uniform coefficients and spatial weighting based on the power density distribution function.

---

[10] J. M. Hendrie and H. J. C. Kouts, Preliminary Hazards Summary Report on the Brookhaven High Flux Beam Research Reactor.

B. Undersea Application of Nuclear Power

A preliminary design was completed for a 2000-shp power plant having a highly enriched pressurized water reactor as the heat source. The purpose of the plant is to propel a 100-ft-long, 15-ft-maximum-diameter submergible research vessel. The ground rules on which the design is based are: (1) present-day technology is employed, and (2) the minimum size of plant is desired.

The major components of the power plant are shown in the flow diagram (Figure 16) and some of the design data in Table XV.

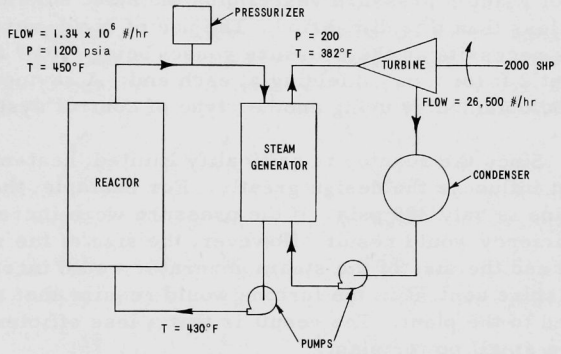

Figure 16. Schematic Diagram for a Pressurized Water Reactor Propulsion System for Underwater Application

Table XV. Design Data

Thermal Power, Mwt	7.75
Shaft Horsepower	2000
Overall Efficiency, %	19.3
Core Dimensions, in.	
Diameter	20
Height	22
PressureVessel Dimensions, ft	
Diameter	4
Height	9
Pressurizer Dimensions, ft	
Diameter	~4
Height	~5
Steam Generator, ft	
Diameter	4.5
Height	10
Turbine Dimension, ft	~4 x 4 x 5
Condenser, ft	
Diameter	~4
Height	~10
Piping	
Outside Diameter, in.	11.2
Length, ft	150

From the study it is believed that a few general observations can be made about pressurized water systems:

(a) Pressurized water reactors pass from a heat-transfer-limited region to a criticality-limited region as the design power decreases below 10-20 Mwt. Therefore, criticality considerations were most important in this design. Accordingly, a conservative heat transfer analysis was performed for the reactor core. Savings in the size of the reactor most likely will be found in the reactor physics aspects rather than in the heat transfer aspects.

(b) Because the maximum diameter of the research vessel is 15 ft, the height of reactor pressure vessel plus the axial shielding is limited to something less than this dimension. The use of rigid, vertical control rod assemblies necessitates the pressure vessel being 8 to 9 ft in height, which allows about 2 ft for axial shielding at each end. A saving in height of about 2 ft could be obtained by using another type of control system.

(c) Since the reactor is criticality limited, heat-removal considerations do not influence the design greatly. For example, the steam pressure at the turbine is only 200 psia. If the pressure were increased, a greater turbine efficiency would result. However, the size of the reactor would not be reduced and the size of the steam generator would increase. Also the higher moisture content in the turbine would require that a moisture separator be added to the plant. The result is that a less efficient steam cycle allows for a small power plant.

C. Conduction-cooled Reactor as a Substitute for an Isotope Heat Source

The limited supply of relatively long half-life isotopes having a reasonably high power density and the low conversion efficiencies attainable with thermoelectric devices has so far limited the power output of isotope-fueled power sources to several tens of watts. In addition, the high cost of the available isotopes would result in a very large expense for isotope-fueled generators producing several hundred watts. It is proposed that a small, minimum-weight reactor, cooled by conduction, would be an attractive alternate to the isotope-powered units in the several hundred watt size range. Accordingly, this study is directed toward the selection of a fuel and moderator for such a reactor system and the preliminary design of the electrical converter and radiator (the latter for a space environment). The nominal size of the power plant is 200 w electric. With a thermoelectric conversion efficiency of 4%, this requires a reactor thermal output of 5000 w.

1. Physics

Critical radius problems for reflected and unreflected, as well as moderated and unmoderated, systems have been run with the aid of the

DSN code for U^{233}, U^{235}, and Pu^{235} fuels. Based on these results, the U^{233} systems with beryllium reflectors look interesting because it is possible to reduce the core mass to as low as 10.5 kg.

2. Radiator Design

The calculations for a tapered cylindrical fin radiator which were programmed on the Pace analog computer have been completed. The results are tabulated in Table XVI.

Table XVI. Summary of Calculations for a Tapered Cylindrical Fin of Beryllium

Base Temperature (°K)	Base* Thickness (cm)	Outer Radius (cm)	Total Power Dissipated (w)	Specific Power Dissipation (w/gm)
600	1.5	42	2950	0.240
600	2.25	42	3400	0.190
600	3.0	52	4510	0.124
600	4.5	52	5700	0.090
700	1.5	32	3550	0.522
700	2.25	42	5250	0.294
700	3.0	42	5900	0.249
700	4.5	52	8400	0.140

*thickness at outer radius = 0.05 cm for all fins

The results of the radiator calculations showed a performance gain (increase in specific power dissipated) of about 1.6 for a tapered fin over a straight fin.

3. Overall System Optimization

From a curve of radiator weight vs radiator temperature a minimum radiator weight of 16.2 kg at a temperature of 620°K was found. This result is for a constant hot-junction temperature for the thermoelectric material of 866°K. This result means that it is possible to have a reactor-thermoelectric system which has a total weight of about 50 kg (excluding shielding) producing 200 w of electric power.

D. Studies of Direct Conversion

1. Measurement of Cesium Ion Currents

In thermionic converters, it is desirable to achieve higher output to neutralize the negative space charge in this cell with positive ions. These ions are usually produced by contact of neutral metal atoms in the vapor (either cesium or potassium vapor) with the hot emitter.

The Saha-Langmuir equation is used to calculate α, the ratio of ions to the total number of ions and neutral atoms, as a function of emitter temperature T_E, atomic density n, ionization voltage, and work function of emitter. The atomic density n is obtained from statistical theory.

The following calculations were based on a tantalum emitter, a cesium vapor work function of 4.1 ev, an ionization voltage of 3.87 ev, and emitter temperatures up to 2033°K.

The expression for the expected saturated ion current J per unit area with cesium is

$$J/cm^2 = 3.315\, n_{cs} \times 10^{14} \sqrt{T_{cs}}\, m\alpha \quad ,$$

where

$\alpha = 0.655$;

T_{cs} = cesium vapor temperature, °K ;

n_{cs} = density of cesium atoms .

The density n_{cs} is determined by the temperature of the cesium trap. In the experiment, however, it takes about an hour to reach equilibrium density in the trap; unfortunately, the trap temperature does not remain constant while the cell is being operated. Since a small change in T_{cs} results in a large change in n_{cs}, it is possible that the difference between the calculated and experimental values may vary as much as an order of magnitude.

The measurements of the saturation currents were made with an X-Y recorder, with a negative voltage, varying from zero to 500 v, applied to the collector and with the emitter at ground. The collector was surrounded by a guard ring. The value of T_{cs} was kept as constant as possible, and the emitter temperature was varied for each measurement. Saturation current was assumed when the recorded current remained essentially constant.

Theoretically, the ion current should be independent of T_E. Actually, an increase in ion current was observed with increasing T_E. The measured and calculated values for the ion current are given in Table XVII.

Table XVII. Variation of Ion Current with Emitter Temperature

T_E, °K	T_{cs}, °K	J/(cm²)(mα) Calculated	J/(cm²)(mα) Measured
1400	336	0.33	0.079
1593	335	0.215	0.110
1723	335	0.203	0.103
1763	330	0.143	0.120
1833	330	0.140	0.205
1968	333	0.146	0.237
2033	335	0.194	0.473

2. Regenerative Emf Cells

Thermally regenerative electrochemical cells which, in a closed cycle, would have the net effect of converting heat from a nuclear reactor or from some other source into electricity are being investigated. Two types of cells are being studied: (1) the lithium hydride cell and (2) bimetallic cells. In all cells tested thus far, liquid lithium metal has been the anode component and mixtures of molten salts containing the lithium ion have served as electrolytes. The two types of cells differ in two respects. In the lithium hydride cell, the cathode component is a gas (hydrogen), whereas in the bimetallic cells the cathode component is a liquid metal. The cells also differ in the phase in which the cell product is deposited. In the lithium-hydrogen cell, the product lithium hydride is formed in the electrolyte and is distributed between the molten electrolyte and the molten lithium metal. In the bimetallic cells, the product appears in the molten cathode metal, and the emf of the cell is simply that of a concentration cell.

In the development of the lithium hydride cell, the first cathode to be investigated consisted of a thin (10-mil) Armco iron diaphragm through which the hydrogen diffused into the molten salt electrolyte. The current density obtained with this cell (about 2 amp/sq ft at 400°C) was considerably smaller than the current density needed to make the cell of practical importance (about 200 amp/sq ft). However, in recent preliminary experiments with vanadium diaphragms, very high solubilities of hydrogen in the metal were noted. It is therefore expected that hydrogen will diffuse through vanadium diaphragms at high rates and that this, in turn, will result in an electrode which is capable of achieving the desired high current density. There are good reasons to expect that other metals, such as niobium, will also prove to be useful diaphragm materials.

Since the diffusion rate of hydrogen through the diaphragm is the predominant factor limiting the power that can be drawn from the lithium hydride cell, an effort was made to increase the diffusion rate by ionizing the hydrogen behind a diaphragm (iron) by means of an alpha source. With a uranium-233 alpha source of about 5×10^8 d/min, the rate of diffusion of hydrogen through a 10-mil-thick iron diaphragm at 400°C and one atm differential hydrogen pressure was found to be about 0.09 cc/min as compared with a rate of 0.05 cc/min without the alpha source (see ANL-6543, page 199).

The bimetallic cells that are currently being studied may be represented as follows:

M_1 (liquid)	Fused salts with M_1 salt in solution	Liquid alloy of M_1 with M_2

where M_1 and M_2 are two metals. Cells of this type offer the possibility of comparatively high current densities at the electrodes in systems that are quite compact. In preliminary experiments with bimetallic cells (see ANL-6543, page 203), the following results were obtained:

System	Temperature Range (°C)	Open-circuit Voltage (v)	Current Density (Anode) at 0.3-v output (ma/sq cm)
Li-Te	496 ± 5	1.9380	475
Li-Bi	489 ± 2	0.9306	650
Li-Sn	450 ± 10	0.7891	450
Li-Pb	483 ± 9	0.6866	270
Li-Zn	468 ± 6	0.6754	225
Li-Cd	493 ± 20	0.6594	385

Further experimentation with bimetallic cells is being planned to yield thermodynamic data. A new liquid metal emf cell has been constructed for this purpose. In the new cell, liquid lithium and various lithium alloys will be contained in covered, porous beryllia crucibles which will be in contact with the fused salt electrolyte. The electrolyte will be contained in a covered tantalum crucible. In addition to the liquid cathode materials previously mentioned, selenium, gallium, thallium, and indium will also be studied.

All the cell systems under study employ materials which are not compatible with ordinary atmosphere. To be successful, experiments must be carried out in an inert atmosphere (helium or argon) in which the concentrations of nitrogen, oxygen, water vapor, and other reactive gases are

in the range of one to 50 ppm. A helium-purification system has been assembled which is capable of maintaining the desired purity of the helium atmosphere. The sequence of steps in the purification system are as follows: the contaminated helium gas flows into a palladium catalytic unit in which hydrogen is converted into water vapor. The water vapor is removed by means of a Molecular Sieve dryer. All remaining contaminant gases in the helium stream are removed in an activated carbon bed cooled by liquid nitrogen (see ANL-6543, page 196).

V. NUCLEAR SAFETY

A. TREAT

1. Operation and Maintenance

RED Test Series 35 was completed, and the samples were returned to Argonne, Illinois, for postmortem examination. This series consisted of four pre-irradiated EBR-II-type fuel pins in a helium environment.

CEN Metal-Water Reaction Test Series 24, consisting of four samples, was completed, and two samples from Series 25 were irradiated. These six samples were aluminum-clad uranium-aluminum alloy plates in room-temperature water. The remaining three samples of Series 25 are at the TREAT site and will be irradiated the first week in December.

2. Installation of Sodium Loop

The feeder from the reactor building service entrance to the Sodium Loop switchgear was installed. Connection of wiring between the switchgear and the step-down transformers used to supply power to the heater circuits for the loop is in progress.

The instrument panels for the loop were installed in the sodium equipment room and on the main floor of the reactor room. Connection of wiring between the instrument panels and the rectifier for the electromagnetic pump is in progress.

Five bellows-type expansion joints for the loop were leak tested and two of the five have been returned to the manufacturer for repair or replacement.

B. Thermal Reactor Safety Studies

1. Metal Oxidation and Ignition Studies

An experimental method is being developed for the study of the oxidation of uranium by air at temperatures above 700°C. In this method, one-cm cubes of uranium will be supported on thermocouples and heated by an external induction coil. Mixtures of air and argon will be passed over the heated sample, and the depletion of oxygen and nitrogen in the effluent gas will be measured continuously by a mass spectrometer. Studies at lower temperatures (300 to 700°C) have indicated that the oxide films produced at high temperatures (above 450°C) are protective against further oxidation. The nature and degree of the protection will be determined in the present study. An important feature of this program will be the assessment of the role of nitrogen in the oxidation reaction.

X-ray diffraction studies of oxidized uranium surfaces have shown that the transition to a protective oxide at 450°C may be related to the absence of oxides higher than uranium dioxide at temperatures above 450°C (see Progress Report, September 1962, ANL-6619, page 57). X-ray examinations of uranium surfaces containing from 400 to 1100 μg O_2/sq cm have now been completed for specimens oxidized at 100, 200, 300, 400, 500, and 600°C. Diffraction patterns showed relatively sharp uranium dioxide lines at 500 and 600°C and somewhat asymmetric diffuse lines at 400°C and below.

An additional experiment was carried out during the present series of isothermal uranium oxidations in the "heat sink" reaction cell (see Progress Report, May 1962, ANL-6573, page 51). The "heat sink" apparatus prevents excessive self-heating of the alloy during the oxidation by pressing the specimen cubes of alloy between large pieces of metal. In the present experiment, uranium was oxidized at 400°C by oxygen that had been dried over phosphorus pentoxide. Preliminary data indicated that the reaction rate was identical with rates determined in experiments in which tank oxygen containing about 50 ppm H_2O was used. It therefore appears unlikely that traces of moisture are the cause of the accelerating rapid rates obtained with uranium below 450°C (see Progress Report, October 1962, ANL-6635, page 55).

Ignition studies of plutonium alloys in air and oxygen are continuing. Burning-curve ignition experiments are being carried out in air with a series of plutonium alloys containing a nominal 2 a/o of additives. The following ignition temperatures were obtained with 0.5-cm cubes: pure plutonium, 520°C; aluminum alloy, 590°C; iron alloy, 548°C; chromium alloy, 512°C; cerium alloy, 510°C; and nickel alloy, 490°C.

2. Metal-Water Studies

Studies of the aluminum-water reaction by the levitation melting method are continuing (see Progress Report, October 1962, ANL-6635, page 56). The experiments consist of suspending a ball of aluminum in an atmosphere of steam by means of a radiofrequency field. The aluminum is then rapidly heated to the test temperature and maintained at this temperature for a period of time. The extent of reaction is obtained by a gravimetric determination of the amount of aluminum oxide (Al_2O_3) produced. Preliminary results have shown that a linear rate law is followed between 1400 and 1600°C. An activation energy of about 50 kcal/mole and a pre-exponential factor of about 4.2×10^5 mg Al/(sq cm) (min) was indicated. Experiments at 1200 and 1300°C indicated that the reaction can be described by a cubic rate law at these lower temperatures. Reaction rates, however, were approximately one-half of those obtained in the range from 800 to 1200°C by the pressure-pulse method (see ANL-6333, page 221). No reason has yet been found for this discrepancy.

In the study of the reaction of uranium with steam by the volumetric method, steam at one atm is passed over metal cubes supported on a thermocouple. Steam in the effluent is condensed and the hydrogen generated by metal-water reaction is measured volumetrically. It was reported previously (see Progress Report, September 1962, ANL-6619, page 57) that results at 1400 and 1500°C were not consistent with the parabolic rate law which was applicable up to 1200°C. The reaction at 1400 and 1500°C appeared to follow a rate law intermediate between a linear and a parabolic rate law. The data show a $\frac{3}{2}$-power law. It seemed likely that a low steam flow rate (10 g/min) might have impeded the rapid initial reaction which is characteristic of oxidation according to a parabolic rate law. Runs at 1400°C were therefore repeated with a high steam-flow rate (about ten times the previous flow rate). Rates at the high steam-flow rate were identical with the previous rates. Visual observation of the reaction showed that the protective oxide developed cracks at random times. Cracking resulted in accelerated local reaction, local temperature excesses, and an overall increase in reaction rate.

In-pile studies of metal-water reactions in the TREAT facility are continuing. In five experiments, 60-mil-thick, 0.5-in. by 1.4-in plates containing a 20-mil-thick core of aluminum-23 w/o uranium (fully enriched) alloy and clad with 20-mil 2S aluminum were subjected to nuclear bursts supplying energies of 174, 245, 361, 430, and 652 cal/g of plate. These plates reacted with the water present in each experiment to the extent of 0.10, 0.13, 0.30, 3.9, and 10.4 percent, respectively. The xenon-133 released to the gas in each assembly was determined and was found to be 0.02, 0.02, 2.8, 27.7, and 35.6 percent, respectively, of the xenon-133 produced by the fission process.

Three experiments with an aluminum-17 w/o uranium (fully enriched)-2 w/o nickel alloy plate with the dimensions of 0.2 by 0.5 by 0.5 in. were performed. The plates were subjected to nuclear bursts which imparted fission energies of 288, 581, and 672 cal/g of plate. These plates reacted with the water to the extent of 0.1, 16.4, and 19.7 percent, respectively. The xenon-133 released to the gas in the experimental assemblies was determined to be 0.6, 38.0, and 35.1 percent, respectively, of the xenon-133 produced by fission. No explosive pressure rises were recorded in any of the experiments.

C. Fast Reactor Safety Studies

1. Temperature Analysis of Experiments with EBR-II Elements Contained in Stagnant Sodium

A total of 20 transient tests in TREAT were run with EBR-II specimens contained in a stagnant sodium annulus with approximately the same cross-sectional areas of sodium around an EBR-II element in an

EBR-II subassembly. Results were reported in previous progress reports (ANL-6409, ANL-6433, and ANL-6525). Transient temperatures were predicted by means of the RE-147 heat transfer code "CYCLOPS." However, the analysis of the experimentally measured temperatures was done with the newer, more versatile code RE-248 "ARGUS" (see Progress Report, September 1962, ANL-6619), since it could mock up the experimental arrangement. The calculations were done to check the experimental consistency of the profiles of the transient radial temperatures, the performance of sample thermocouples; and the temperature rise recorded by fast-response thermocouples on the outside of the steel tube containing the sodium bath.

Briefly, the results with 3% enriched elements are summarized. For transients initiated with an excess reactivity (k_{ex}) of 1.5% (initial reactor period of 0.11 sec) and clipped with control rods to yield preprogrammed energy releases, reactor energy releases in the range from 140 to 170 Mw-sec tended to produce small areas of fuel-cladding alloying, but not failure. Calculated maximum fuel temperatures were in the melting range (1010-1100°C), and maximum fuel-cladding interface temperatures were in the approximate range from 850 to 950°C for 140- to 170-Mw-sec tests. A release of 180 Mw-sec established the threshold for extensive failure.

The calculations are in reasonable agreement with previous in-pile meltdown tests, if the fuel-cladding interface temperature is used as a criterion. Transient temperatures recorded from thermocouples on the steel tube containing the sample and sodium showed no heat loss from the tube over a time scale of the order of a few seconds. Measured tube temperature rises although showing some scatter, could be correlated linearly with reactor energy release.

The sample power-reactor power calibration factor when compared with one obtained by radiochemical analysis of a low power calibration sample was about 16% lower than that needed to reconcile the isothermal adiabatic temperature rise for a sample-sodium-tube system. Hence, a new "experimental" calibration factor, 16% greater than the radiochemical value, was used in the detailed calculations. (This experimental value was about 10% lower than the preliminary calibration established by correcting results from experiments with uncooled samples for the effect of the sample container on the thermal neutron flux.) Transient tube temperature rises had the same shape as calculated, indicating no evidence of appreciable interference in heat transfer between the sample element and container tube. Thus there is no evidence for expulsion of sodium in a transient from the annulus for at least a period of the order of 0.2 to 0.4 sec.

Results of tests with a natural uranium specimen, subjected to temperature-limited transients, and with four 3% enriched specimens, subjected to a shaped axial power profile typical of that for EBR-II, were in agreement with those calculated for the other tests.

2. Tests with Pre-irradiated Samples in the Absence of Coolant

A series of four tests was performed with EBR-II elements that had previously been irradiated to burnups estimated to be in the range from 0.5 to 1.0 a/o. TREAT irradiation conditions were as follows:

Sample No.	Reactor Integrated Power (Mw-sec)	Maximum Recorded Sample Cladding Temperature (°C)
5	44	790
6	48	860
7	61	930*
8	88	990*

*Indications of perturbations in recording above 900°C

Samples 5 to 7 were subjected to pulses initiated with 1.03% k_{ex} (initial period of 0.25 sec) and clipped by pre-programmed rod scrams. Sample 8 received a constant power transient, initiated on a 2.5-sec period with nominal peak power of 5 Mw, sustained for 11 sec beyond the time of peak power by programmed control rod motion. The samples have been returned to Argonne for remote inspection in the cave facilities.

VI. PUBLICATIONS

Papers

AN ITERATIVE METHOD FOR QUADRATURES
Henry C. Thacher, Jr.
The Computer Journal, Vol. 5, No. 3, pp. 228-229
(October, 1962)

DISCRETE ORDINATE QUADRATURES FOR THIN SLAB CELLS
David Meneghetti
Nuclear Science and Engineering, 11, 295-303
(November, 1962)

MANUFACTURE OF CRACK-FREE, SMALL ZIRCALOY TUBING BY DRAWING ON A DUCTILE, DISPOSABLE CORE
N. H. Polakowski
J. Inst. Metals 91 44-47 (1962)

OXIDATION AND PHASE STABILITY IN SOLID SOLUTION SYSTEMS CONTAINING URANIUM OXIDE
E. D. Lynch
TID-7637, Characterization of Uranium Dixoide, 434-457

NEUTRON RADIOGRAPHY
Harold Berger
Scientific American 207 (5) 107-119

URANIUM POWDER IGNITION STUDIES
M. Tetenbaum, L. Mishler, and G. Schnizlein
Nuclear Sci. and Eng. 14 (3), 230-238 (November, 1962)

The following papers were presented at the American Nuclear Society Winter Meeting, Washington, D. C., November 26-28, 1962

DIRECT REDUCTION OF THORIUM DIOXIDE
A. V. Hariharan, J. B. Knighton, R. K. Steunenberg
Trans. Am. Nuclear Soc. 5 (2), 461-462 (November, 1962)

FILTRATION OF VAPOR-PHASE HYDROLYZED PLUTONIUM HEXAFLUORIDE
R. Kessie, J. Fischer, and T. Gerding
Trans. Am. Nuclear Soc. 5 (2), 458-459 (November, 1962)

DISTRIBUTION OF SELECTED ELEMENTS BETWEEN MAGNESIUM CHLORIDE AND MAGNESIUM-ZINC ALLOY
J. B. Knighton, and R. K. Steunenberg
Trans. Am. Nuclear Soc. 5 (2), 460-461 (November, 1962)

A FLUID-BED PROCESS FOR THE DIRECT CONVERSION OF URANIUM HEXAFLUORIDE TO URANIUM DIOXIDE

I. E. Knudsen, H. E. Hootman, and N. M. Levitz

Trans. Am. Nuclear Soc. 5(2), 457 (November, 1962)

SEPARATION OF GASEOUS MIXTURES OF URANIUM HEXAFLUORIDE AND PLUTONIUM HEXAFLUORIDE BY THERMAL DECOMPOSITION

L. E. Trevorrow, J. Fischer, and J. Riha

Trans. Am. Nuclear Soc. 5 (2), 457-458 (November, 1962)

AN ENGINEERING-SCALE HIGH-ALPHA FACILITY FOR STUDIES OF THE PLUTONIUM FLUORIDE VOLATILITY PROCESS

G. J. Vogel, E. L. Carls, W. J. Mecham, and A. A. Jonke

Trans. Am. Nuclear Soc. 5 (2), 326-327 (November, 1962)

Proc. 10th Conf. on Hot Laboratories and Equipment. Am. Nuclear Soc., Chicago, 1962, pp. 287-291

FARÉT - A FAST-REACTOR FACILITY

A. Smaardyk, R. Brubaker, H. Hummel, and A. McArthy

Trans. Am. Nuclear Soc. 5 (2), 435-436 (November, 1962)

MAJOR ACCIDENT STUDIES FOR ZERO-POWER EXPERIMENTAL FAST REACTORS

Sushil K. Kapil and George J. Fischer

Trans. Am. Nuclear Soc. 5 (2), 418-419 (November, 1962)

CRITICALITY BY A ZONE TECHNIQUE FOR FAST-REACTOR SYSTEMS

F. H. Helm

Trans. Am. Nuclear Soc. 5 (2), 353 (November, 1962)

STUDIES OF THE DOPPLER EFFECT IN LARGE CERAMIC-FUELED FAST REACTORS

H. H. Hummel and M. G. Bhide

Trans. Am. Nuclear Soc. 5 (2), 366-367 (November, 1962)

USE OF DEPLETED URANIUM IN THERMAL REACTORS WITH SLIGHTLY ENRICHED FUEL TO ACHIEVE HIGH NEUTRON, ECONOMY AND BURNUP

Haig P. Iskenderian

Trans. Am. Nuclear Soc. 5 (2), 356-357 (November, 1962)

ADVANCED HIGH-FLUX RESEARCH REACTOR TECHNOLOGY

C. N. Kelber, B. I. Spinrad, and L. J. Templin

Trans. Am. Nuclear Soc. 5 (2), 425-426 (November, 1962)

EXPERIMENTS TO COMPARE RADIATION DAMAGE DOSE RATES IN DIFFERENT REACTOR SPECTRA
A. D. Rossin
Trans. Am. Nuclear Soc. 5 (2), 472 (November, 1962)

THE ELASTIC SCATTERING OF FAST NEUTRONS FROM U^{235} AND U^{238}
A. B. Smith and D. Reitmann
Trans. Am. Nuclear Soc. 5 (2), 363-364 (November, 1962)

A FORTRAN-II SUBROUTINE TO CALCULATE HYDROGEN PROPERTIES FOR NUCLEAR ROCKET STUDIES
Gerald H. Golden and Charles E. Cohn
Trans. Am. Nuclear Soc. 5 (2), 433-434 (November, 1962)

DIGITAL METHOD FOR CONTROL ROD CALIBRATION
Charles E. Cohn and Jerry J. Kaganove
Trans. Am. Nuclear Soc. 5 (2), 388-389 (November, 1962)

MECHANICAL DECANNING OF EBR-II FUEL ELEMENTS
J. P. Simon and J. R. White
Proc. Hot Lab. & Equip. Conf., 10th, 91-98, published by The American Nuclear Society, Chicago (1962).
Trans. Am. Nuclear Soc. 5 (2), 306 (November, 1962)

EBR-II FUEL DISMANTLING EQUIPMENT
J. P. Simon and R. B. Wehrle
Proc. Hot Lab. & Equip. Conf., 10th, 99-110, published by The American Nuclear Society, Chicago (1962).
Trans. Am. Nuclear Soc. 5 (2), 305-306 (November, 1962).

FIRE AND EXPLOSION TESTS OF PLUTONIUM GLOVEBOXES
H. V. Rhude
Proc. of the 10th Conf. on Hot Laboratories & Equipment, Nov. 26-28, 1962, 305-311. Trans. Am. Nuclear Soc. 5 (2), 328 (November, 1962)

ANL REPORTS

ANL-6314 CERAMIC NUCLEAR FUELS IN THE SYSTEM ZrO_2-CaO-UO_2
J. H. Handwerk, G. D. White, and D. C. Hill

ANL-6319 Rev. ENGINEERING APPLICATIONS OF ANALOG COMPUTERS
Lawrence T. Bryant, Marion J. Janicke, Louis C. Just and Alan L. Winiecki

ANL-6551 A PROCEDURE FOR THE EVALUATION OF NEUTRON-SCATTERING CROSS SECTION IN THE INCOHERENT APPROXIMATION
V. Z. Jankus

ANL-6614 EXPERIMENTAL BREEDER REACTOR-II (EBR-II) SHIELD DESIGN
M. Grotenhuis, A. E. McArthy, and A. D. Rossin

ANL-6629 CORE A CRITICAL STUDIES FOR THE ENRICO FERMI ATOMIC POWER PLANT ON ZPR-III
C. E. Branyan